

**REGULATION OF INTEGRIN- α_M AND - β_2 EXPRESSION ON THE
SURFACE OF MACROPHAGES IN RESPONSE TO INFECTION
WITH *Mycobacterium avium*.**

by

MAURICE AYAMBA ITOE

Supervisor: Prof. Lutz Thilo

PRESENTED IN FULFILMENT FOR M.Sc (MED) DEGREE IN
MEDICAL BIOCHEMISTRY, DIVISION OF MEDICAL
BIOCHEMISTRY, UNIVERSITY OF CAPE TOWN

September, 2007

The copyright of this thesis vests in the author. No quotation from it or information derived from it is to be published without full acknowledgement of the source. The thesis is to be used for private study or non-commercial research purposes only.

Published by the University of Cape Town (UCT) in terms of the non-exclusive license granted to UCT by the author.

DECLARATION

I, MAURICE AYAMBA ITOE, hereby declare that the work on which this thesis is based is my original work (except where acknowledgements indicate otherwise), and that neither the whole work nor any part of it has been, is being, or is to be submitted for another degree in this or any other university.

I empower the University of Cape Town to reproduce for the purpose of research either the whole or any portion of the contents in any manner whatsoever.

Signature

12-11-2007
Date

ACKNOWLEDGEMENTS

I will ever be grateful to the following people:

- Prof. Lutz Thilo for his interest in my development as a scientist.
- Dr. Chantal de Chastellier (Universitaire de Marseilles) for her assistance in producing the electron microscopy pictures.
- Dr. Christopher Maske for his technical assistance in my immunofluorescence experiments.
- Prof. Dave Marais and members of the Lipid laboratory, Division of Medicine, University of Cape Town, for their technical assistance.
- Medical Research Council of South Africa for funding this project.
- My laboratory colleagues Raydean Pietersen and Roshan Ebrahim for their moral support.
- My parents for moral and financial support.
- My son Bakoma N. Itoe, whose coming eleven months ago really inspired me to work even harder.
- My wife, Chantal, for her love and support.
- My flat mates Cyprian, Jan, Anne and my friend Graham Rowe were of invaluable encouragement throughout my studies at the University of Cape Town.
- God almighty for the strength.

SUMMARY

Tuberculosis continues to be a major public health problem globally with over a third of the world's population latently infected and close to 3million deaths reported annually. The high prevalence of the disease owes to the fact that the causative agent, *Mycobacterium tuberculosis*, is able to survive and replicate within host macrophages whose main function is to destroy invading pathogens. *M. avium*, an avian pathogen, can be pathogenic to humans who are immuno-compromised. Inside macrophages, the pathogenicity of mycobacteria correlates with a modified composition of the enclosing phagosome membrane. On the cell surface, the expression of integrin- α_M and integrin- β_2 is altered when determined by exo-galactosylation with radioactive galactose (Itoe, B.Sc(med)Honours thesis, 2004). These integrins exist as a heterodimer to form Mac-1 or CR3 receptor.

This project was aimed at determining the mechanism(s) of integrin- β_2 down-regulation and concurrent up-regulation of integrin- α_M on the surface of macrophages in response to infection with mycobacteria and to identify the factor(s) responsible for the change. It also aimed at identifying a possible alternative dimerization partner of integrin- α_M in the context of reduced surface expression of integrin- β_2 . The observed changes of integrin surface expression could come about by a redistribution from plasma membrane to intracellular pools or by a change in the transcriptional level of integrin- α_M and integrin- β_2 genes. This was tested by Western blot, RT-PCR and immunofluorescence analyses.

Western blot analysis of total membrane protein for the abundance of integrin- β_2 showed no difference at the protein level between *M. avium*-infected and uninfected cells.

In order to confirm or refute this finding, a quantitative RT-PCR experiment was performed using pairs of primers specific for mouse integrin- α_M and integrin- β_2 genes. No significant difference was observed at the mRNA level for integrin- α_M and - β_2 gene expression between *M. avium*-infected and uninfected cells.

To observe whether altered surface expression was the result of a redistribution between the cell surface and intracellular membranes, a semi-quantitative immunofluorescence analysis was done. No significant differences were observed when comparing *M. avium*-infected and non-infected cells for both surface and intracellular pools of integrin- α_M and integrin- β_2 .

To obtain a more sensitive measure for a possible redistribution, the accessibility for surface radiolabelling was compared. A 2-fold decrease of integrin- β_2 label was observed for infected cells when relating radiolabel with Western blot band intensity.

The altered surface expression of integrin- α_M and integrin- β_2 could be induced in non-infected macrophages when these were exposed to medium that had been conditioned by infected cells.

Co-immunoprecipitation experiments using purified anti-integrin- α_M monoclonal antibody did not show up any alternative dimerisation partner for integrin- α_M despite the declining abundance of integrin- β_2 on the cell surface.

In conclusion, our results indicate that infection of macrophages with *M. avium* caused a redistribution of integrin- β_2 between the plasma membrane and intracellular membranes. In spite of this effect, no additional dimerization partner was observed to compensate for the declining abundance of integrin- β_2 on infected cells.

CONTENTS

Chapters	Page
Acknowledgements	i
Summary	ii
Contents	iv
1. Introduction	1
1.1 Tuberculosis infection	1
1.2 Macrophages in cell immunity	3
1.2.1 Uptake and processing of non-pathogenic particles	3
1.2.2 Processing of pathogenic mycobacteria	4
1.3 The CR3 and Mac-1	9
1.3.1 Genes, biology, structure and functional domains	9
1.3.2 Role of CR3 in cell immunity	11
1.4 Thesis question	13
2. Results chapter	16
2.1 Optimisation of methods	16
2.1.1 Immunofluorescence for comparing cell surface integrins	16
2.1.1.1 Optimisation of antibody dilutions	16
2.1.1.2 Specificity of staining with anti-integrin- α_M antibody M1/70	17
2.1.2 Western blot conditions for semi-quantitative detection	18
2.1.2.1 Dilution of anti-integrin- β_2 antibody C71/16	18
2.1.2.2 Dilution of anti-integrin- α_M polyclonal antibody M-19	21
2.1.3 RT-PCR conditions for measuring integrin gene expression	22

2.1.3.1 Quality of isolated RNA	22
2.1.3.2 Specificity of designed primers	23
2.1.4 Determination of optimal cell count needed for co-immunoprecipitation of integrin- β_2 with $-\alpha_M$	24
2.2 Results	26
2.2.1 Macrophages contained actively replicating and viable bacteria	26
2.2.2 Labelling of plasma membrane glycoconjugates	27
2.2.3 SDS-PAGE of ^{14}C -labelled plasma membrane	29
2.2.4 Trypsin ingel digestion for ^{14}C - and ^3H -labelled plasma membrane	31
2.2.5 Does the decrease in integrin- β_2 occur at a transcriptional or translational level?	32
2.2.6 Differential surface expression of integrin- α_M and integrin- β_2 on macrophages in response to infection with <i>M. avium</i>	36
2.2.7 Comparative whole cell staining for integrin- β_2 and $-\alpha_M$ in <i>M. avium</i> -infected and non-infected macrophages	38
2.2.8 Infection of macrophages with <i>M. avium</i> causes a redistribution of integrin- β_2 between the plasma membrane and intracellular pools	41
2.2.9 Integrin- α_M co-immunoprecipitates with integrin- β_2 in <i>M. avium</i> -infected macrophages	44
2.2.10 Culture medium from <i>M. avium</i> -infected macrophages causes an altered surface expression of integrin- α_M and $-\beta_2$ on non-infected macrophages	46
3. Discussion	48
3.1 Implication of results	53

3.2 Conclusion and future perspectives	54
References	56
Chapter 4 Materials and Methods	70
4.1 Harvesting of mouse bone marrow-derived macrophages and cell culturing	70
4.2 Culturing and storage of <i>Mycobacterium avium</i>	71
4.3 Infection of macrophages with <i>M. avium</i>	71
4.4 Preparation of <i>M. avium</i> -infected cells for electron microscopy	72
4.5 Labelling and isolation of plasma membrane glycoproteins	72
4.5.1 Protein quantification assays	74
4.5.1.1 Bio-rad protein assay	74
4.5.1.2 Bicinchoninic acid (BCA) protein assay	75
4.6 Protein electrophoresis	76
4.6.1 Gradient SDS-PAGE for determination of radioactivity profiles of labelled plasma membrane protein	76
4.6.1.1 Preparation and pouring of an 8%-15% gradient SDS-PAGE	76
4.6.1.2 Preparation and pouring of the stacking gel	77
4.6.1.3 Loading and separation of proteins	77
4.6.2 Lined SDS-PAGE for Western blotting	78
4.6.2.1 Western blotting	79
4.7 Visualisation of protein bands on SDS-PAGE by Coomassie Brilliant Blue staining protocol	80
4.8 Autoradiography	81
4.9 Trypsin ingel digestion	81

4.10 RNA isolation from uninfected and <i>M. avium</i> -infected mouse bone marrow-derived macrophages	82
4.10.1 Determination of RNA concentration	83
4.10.2 Checking the integrity of RNA obtained	83
4.10.3 Single strand (cDNA) synthesis	84
4.11 Bioinformatics	84
4.12 Quantitative Real time Reverse Transcription Polymerase Chain Reaction (qRT-PCR)	85
4.12.1 Synthesis of primers	85
4.12.2 Real time Reverse transcriptase polymerase chain reaction (Real time RT-PCR) - cDNA amplification	85
4.12.3 DNA electrophoresis of PCR products	86
4.13 Immunofluorescence	87
4.13.1 Surface staining of integrin β_2 and α_M on <i>M. avium</i> -infected and non-infected macrophages	87
4.13.2 Intracellular staining of integrin- β_2 and α_M in <i>M. avium</i> -infected and uninfected mouse bone marrow-derived macrophages	88
4.14 Co-immunoprecipitation of ^{14}C -labelled $\alpha_M\beta_2$	89
4.15 Filtration of medium from <i>M. avium</i> -infected cells and transfer onto non-infected cells	90

INDEX FOR FIGURE TITLE

Figure	Page
Figure 1 Changes in surface expression of integrin- α_M (peak A3) and integrin- β_2 (peak A4) on mouse bone marrow-derived macrophages in response to Infection with <i>M. avium</i>	9
Figure 2 Staining with different dilutions of anti-integrin- β_2 antibody	17
Figure 3 Specificity of staining with Alexa 488-conjugated anti-integrin- α_M antibody M1/70	18
Figure 4A Optimisation of Western blot conditions for anti-integrin- β_2 antibody	19
Figure 4B Densitometry analysis for optimisation of anti-integrin- β_2 antibody dilutions in Western blots	20
Figure 5 Western blots conditions for anti-integrin- α_M polyclonal antibody M-19	22
Figure 6 Quality of RNA isolated from <i>M. avium</i> -infected and uninfected mouse bone marrow-derived macrophages	23
Figure 7 Analysis of test PCR products on 2% agarose gel	24
Figure 8 Co-immunoprecipitation of ^{14}C -surface-labelled $\alpha_M\beta_2$	25
Figure 9 Thin sections of <i>M. avium</i> -infected mouse bone marrow-derived macrophages	26
Figure 10 Partitioning of labelled plasma-membrane glycoprotein by density centrifugation on 27% Percoll gradients	28
Figure 11 SDS-PAGE of membrane proteins	30
Figure 12 Differential cell-surface expression of glycoproteins on <i>M. avium</i> -infected (7days post-infection) and non-infected macrophages	32
Figure 13 Comparative expression of integrin- β_2 in macrophages, with or without infection with <i>M. avium</i>	33
Figure 14 Expression of integrin- β_2 and - α_M genes of mouse bone marrow-derived upon infection with or without <i>M. avium</i>	34
Figure 15 Polymerase chain reaction amplification of integrin- α_M and - β_2 genes from <i>M. avium</i> -infected and non-infected mouse bone marrow-derived macrophages	35

Figure 16 Differential surface expression of integrin- α_M on macrophages in response to infection with <i>M. avium</i>	37
Figure 17 Differential surface expression of integrin- β_2 on macrophages in response to infection with <i>M. avium</i>	37
Figure 18 Cell-surface fluorescence intensity for integrin- α_M and integrin- β_2 in <i>M. avium</i> -infected and non-infected macrophages	38
Figure 19 Intracellular expression of integrin- α_M in macrophages response to infection with <i>M. avium</i>	39
Figure 20 Intracellular expression of integrin- β_2 in macrophages response to infection with <i>M. avium</i>	40
Figure 21 Intracellular fluorescence intensity for integrin- α_M and integrin- β_2 in <i>M. avium</i> -infected and non-infected macrophages	40
Figure 22 Western blotting followed by autoradiography of ^{14}C -labelled membrane glycoconjugates from <i>M. avium</i> -infected and non-infected cells	42
Figure 23 Intensities versus microgram plots of ^{14}C -labelled membrane proteins from <i>M. avium</i> -infected and non-infected cells	43
Figure 24 Co-immunoprecipitation of $\alpha_M\beta_2$ complex from <i>M. avium</i> -infected and non-infected macrophages with anti-integrin- α_M	44
Figure 25 Analysis of molecular weight of integrin- α_M and - β_2 chains on 7% SDS-PAGE after Co-immunoprecipitation	45
Figure 26 Effect of medium from <i>M. avium</i> -infected cells on the expression of integrin- β_2 and - α_M on non-infected cells	47

INDEX FOR DIAGRAM TITLE

	Page
Diagram 1 Granuloma formation	2
Diagram 2 Features of β_2 integrins	10
Diagram 3 Schematic representation of radiolabelling of cell-surface glycoproteins	15

University of Cape Town

Chapter 1: INTRODUCTION

Tuberculosis continues to remain a major public health problem globally with over a third of the world's population latently infected and close to 3million deaths reported annually (Dye *et al*, 1999). In humans, tuberculosis is caused by the intracellular pathogen *Mycobacterium tuberculosis*. The incidence of the disease has been exacerbated by the emergence of extremely multi-drug resistant strains of the intracellular pathogen. An avian pathogen, *Mycobacterium avium* can also be pathogenic to immunosuppressed individuals as in the case of HIV infection (Rieder *et al.*, 1980; Dye *et al*, 1999).

1.1 Tuberculosis infection

Tuberculosis infection occurs through inhalation of bacteria-containing droplets into the lungs of individuals where they are taken up and harboured by alveolar macrophages. These macrophages are then transported to lymph nodes where a granulomatous lesion develops for the containment of the bacteria. Granuloma formation is the hallmark of tuberculosis disease. It is characterized by a central necrotic core, followed by a layer of blood-derived macrophages, epithelioid cells, multinucleated giant cells and a rim of T lymphocytes (Diag. 1, Russel, 2007). The development of a tuberculous granuloma is controlled by cytokines and chemokines. The infected cells present antigens to T cells and activate them to produce a number of cytokines and chemokines. The chemokines recruit other circulating cells from blood to the site of infection. Interferon γ (IFN γ) from lymphocytes and macrophage-derived tumor necrosis factor (TNF) activate macrophages to kill intracellular mycobacteria (Reviewed by Kaufman, 2002). The lymphocytes are recruited in the following order starting with CD₄ T cells, followed by CD₈ T cells. Flynn

and Chan, (2005) argued that while a reasonable immune response is beneficial for the host in terms of keeping the infection localized and under control, it would ultimately be advantageous for the effective dissemination of mycobacteria.

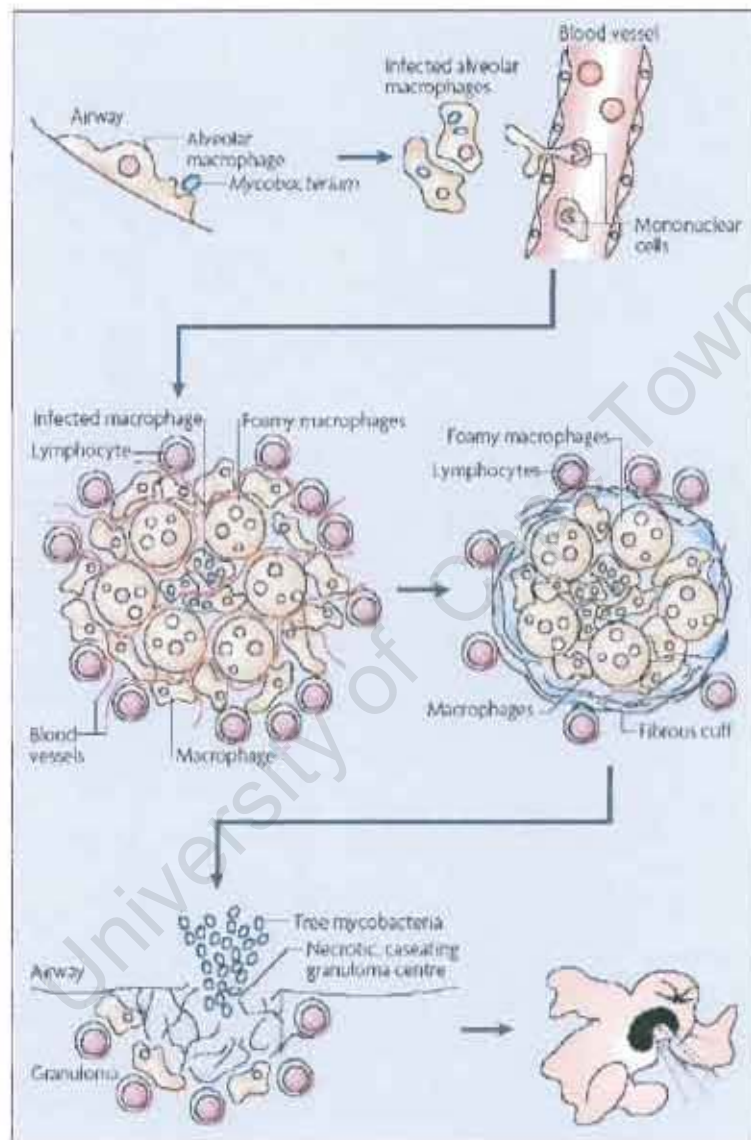


Diagram 1. **Granuloma formation.** Inhaled *M. tuberculosis* enter into lung aveoli macrophages and replicate therein. Inflammatory response leads to recruitment of blood and tissue macrophages and lymphocytes leading to the development of a granuloma. Epithelioid cells are formed from differentiated macrophages. Multinucleated giant cells are formed from fused macrophages. Reproduced from Russell, 2007.

1.2 Macrophages in cell immunity

1.2.1 Uptake and processing of non-pathogenic particles

Phagocytic uptake of particles occurs either by type 1 or type 2 phagocytosis. While type 1 phagocytosis is characterized by pseudopodia extension, type 2 is characterized by sinking of the particle into the cell (Kaplan, 1977). The uptake can either be opsonic or non-opsonic depending on whether or not immunoglobulins or complement factors are bound onto the surface of the bacteria (Allen and Aderem., 1996). Internalisation of particles is mediated by several cell-surface receptors including the complement receptor CR3, mannose receptor and scavenger receptors (Schlesinger, 1993) via specific molecular interactions between bacterial polysaccharides and recognition domains of the receptors (Cywes *et al.*, 1997). These interactions trigger a series of intracellular signals that cause rearrangement of the actin cytoskeleton around the phagocytic particle to form the phagocytic cup. Both ends of the plasmalemma fuse and a plasma membrane-derived vacuole termed a phagosome is formed (Kaplan, 1977; Allen and Aderem, 1996). Soon after uptake of mouse antibody-coated *Staphylococcus aureus* by macrophages, the plasma membrane-derived phagosome fuses with and exchanges membrane with early endosomes (Mayorga *et al.*, 1991; Pitt *et al.*, 1992). Similar observations have also been reported when degradable *Bacillus subtilis* was used as a phagocytic particle (de Chastellier *et al.*, 1995). The early endosomes-like phagosome gradually matures and starts fusing with lysosomes. Upon fusion with lysosomes, the pathogen becomes destroyed by the harsh hydrolytic environment inside lysosomes (Mayorga *et al.*, 1991). Phagosome maturation is a prerequisite for phagosome-lysosome fusion to occur. The maturation process involves a gradual modification of the phagosome by specific addition

and removal of selected proteins of the endocytic pathway (Pitt *et al.*, 1992; Desjardin *et al.*, 1994). The early endosome-phagosome and late endosome-phagosome fusions are mediated by rab5 and rab7 respectively. Both rab5 and rab7 belong to the GTPase super family and are located at different stages and structures of the endocytic pathway where they regulate specific steps of membrane traffic (Chavrier *et al.*, 1990; Bourne *et al.*, 1991). Rab5 is present on both the plasma membrane and early endosomes (Chavrier *et al.*, 1990) where it regulates homotypic fusion between early endosomes/phagosomes and fusion of plasma membrane-derived vesicles with early endosomes (Gorvel *et al.*, 1991; Bucci *et al.*, 1992). It has also been shown to regulate the movement of early endosomes along the microtubule network (Nielsen *et al.*, 1999). On the other hand, rab7 is localized to late endosomes where it regulates late endocytic traffic (Feng *et al.*, 1995; Vitelli *et al.*, 1997). In a more recent study, rab7 has been shown to associate with lysosomes where it mediates their fusion with late endocytic structures (Bucci *et al.*, 2000).

1.2.2 Processing of pathogenic mycobacteria

In contrast, soon after uptake, pathogenic mycobacteria prevent the phagosomes in which they reside from fusing with lysosomes thereby evading the harsh hydrolytic environment inside lysosomes (Armstrong and Hart, 1971; Frehel *et al.*, 1986). Mycobacterium-containing phagosomes behave like endosomes. They continue to fuse and intermingle content and membranes with early endosomes, but not with lysosomes and are often referred to as early endosome-like phagosomes (Clemens and Horwitz, 1995; de Chastellier and Thilo, 2002). Mycobacteria continue to survive and multiply within these phagosomes. To successfully combat the tuberculosis disease, it is necessary

to gain a better understanding of the mechanisms being employed by pathogenic mycobacteria to survive within host macrophages.

Evidence for non-maturation of mycobacterium-containing phagosomes is provided by the presence on mycobacterium-containing phagosomes of early endosomal markers such as transferrin receptor, rab5, but not the late endosomal marker rab7 (Clemens and Horwitz, 1995; Via *et al.*, 1997; Kelley and Schorey, 2003). The continued presence of rab5, but not rab7, on mycobacterium-containing phagosomes (Via *et al.*, 1997; Kelley and Schorey, 2003) suggests that the molecular mechanisms occurring between the stages controlled by rab5 and rab7 are being compromised and that maturation is inhibited.

For more than a decade now, the question has shifted from how pathogenic mycobacteria prevent phagosome-lysosome fusion to how mycobacteria inhibit phagosome maturation. Phagosomes containing hydrophilic latex beads or non-pathogenic particles mature within 5 minutes, after which they start fusing with lysosomes (Pitt *et al.*, 1992; de Chastellier *et al.*, 1995; Oh and Swanson, 1996; de Chastellier and Thilo, 1997). This suggests that any mechanisms by which mycobacteria could be affecting the maturation process must be occurring within minutes after phagosome formation.

Several molecular mechanisms have been proposed for how mycobacterium blocks phagosome maturation.

As opposed to latex beads, mycobacteria exclude recruitment of EEA1 (early endosome autoantigen 1), a rab5 effector, to the phagosomal membrane (Fratti *et al.*, 2001). EEA1 is transiently recruited to the early endosomal/early phagosomal membrane during maturation (Simonsen *et al.*, 1998). EEA1 is a peripheral membrane protein associated with early endosomes (Mu *et al.*, 1995; Patki *et al.*, 1997) through its zinc-binding FYVE domains that interact with both phosphoinositide-3-phosphate (PI3P) and rab5 (Stenmark *et al.*, 1996; Gaullier *et al.*, 1998; Lawe *et al.*, 2000). PI3P is a product of class III PI-3-kinase present on phagosomes (Vieira *et al.*, 2001). EEA 1 facilitates membrane fusion by acting as a tethering molecule between early endosomes (Simonsen *et al.*, 1999). Mycobacterium-containing phagosomes lack proper luminal acidification due to the partial exclusion of the vacuolar H⁺-ATPase (Sturgill-Kosyiki *et al.*, 1994; de Chastellier *et al.*, 1995). They have a lowered level of the v-SNARE, cellubrevin (Fratti *et al.*, 2002). Cellubrevin is a SNARE (Soluble N-ethylmaleimide-sensitive factor attachment protein receptor) molecule that is involved in recycling of plasma-membrane markers from the endosomes (Galli *et al.*, 1994). TACO (tryptophan aspartate-containing coat protein), also known as coronin, is recruited and retained at the phagosomal membrane and released before fusion of phagosomes with lysosomes. Ferrari *et al.* (1999), proposed that the retention of TACO by live but not dead mycobacteria seems to present another strategy being employed by pathogenic mycobacteria to avoid phago-lysosome fusion. However, a more recent report by Schuller *et al.* (2001), contradicts these findings. They showed that TACO, being an actin-binding protein, is only involved in phagocytic uptake but not in the prevention of phagosome maturation. The presence of TACO on phagosomal membranes could be explained by observations where F-actin

filaments were found to assemble around latex bead-containing phagosomes and propelled them towards fusion with other organelles of the endocytic pathway (Desjardins *et al.*, 1994; Defacque *et al.*, 2000; Möller, W., *et al.*, 2000) through the action of an actin comet tail (Taunton *et al.*, 2000). More recent studies by Guérin and de Chastellier (2000) showed that mycobacteria caused a marked disorganization of actin filaments that resulted in a lag in the acquisition of early endosomal marker HRP (Horse-reddish peroxidase) by mycobacterium-containing phagosomes from early endosomes. Also, occurring naturally on phagosomal membrane is a natural resistance associated membrane protein (Nramp1). This protein has a bacteriostatic effect and the mycobacteria are unable to prevent phagosome maturation and fusion with lysosome (Frehel *et al.*, 2002). Only in Nramp1-negative mice can *M. avium* prevent phagosome maturation and fusion with lysosomes.

Studies by de Chastellier and Thilo (1997) suggest that mycobacterium-containing phagosomes only remain immature if there is an all-around close apposition between the phagosomal membrane and the bacterial cell surface. This morphology contrasts with the tubular extension observed for early endosomes and for phagosomes with hydrophilic latex beads. The absence of tubular extensions on the mycobacterium-containing phagosomes suggests that recycling may be impaired, with the tubular extensions being involved in recycling of fusion mediating factors. An all-around close apposition of the phagosomal membrane to the mycobacterial surface would imply the existence of specific molecular interactions between constituents of the phagosomal membrane with those of the mycobacterial surface. This raises the possibility that the phagosome

membrane may have a characteristic composition. It has been shown that the prevention of phagosome maturation correlates with a modified composition of the phagosome membrane in terms of cell surface-derived labelled glycoproteins (de Chastellier and Thilo, 2002; Pietersen *et al.*, 2004). In the course of these studies, it was observed that mycobacterial infection caused a change in the expression of glycoproteins on the macrophage surface.

Recently, we undertook to characterize this altered surface expression in terms of its post-infection time course and the cell-surface glycoproteins involved. Macrophages were infected with *M. avium*. ^{14}C -labelled plasma-membrane proteins were obtained from the macrophages at 1.5 days, 3.5 days and 7 days post-infection. At the same stage of growth, ^3H -labelled plasma-membrane proteins were also isolated from non-infected cells. The ^{14}C -labelled and ^3H -labelled plasma-membrane proteins from each stage were mixed together and analysed in the same lane on an 8%-15% gradient SDS-PAGE. Each lane was divided into 2.5 mm wide slices and subjected to two rounds of trypsinization to release labelled protein fragments. The digestion products from each slice were counted in a liquid-scintillation counter. The amount of radioactivity was plotted against slice number in order to observe how the radioactivity is distributed across the gel. An up-regulation was observed for glycoproteins in the 170-200kDa region and a down-regulation was observed for glycoproteins in the 100kDa region. MALDI-TOF analysis of fractions corresponding to these regions identified the cell-surface proteins integrin- α_{M} (also named CD11b; 40% increase) and integrin- β_2 (also called CD18; 80% decrease with $T_{1/2} \approx 1.5$ days; Itoe, B.Sc Hons dissertation, 2004). Integrin- α_{M} and integrin- β_2 are present on the cell surface as heterodimer, $\alpha_{\text{M}}\beta_2$, otherwise known as Mac-1 receptor. *al.*, 2002).

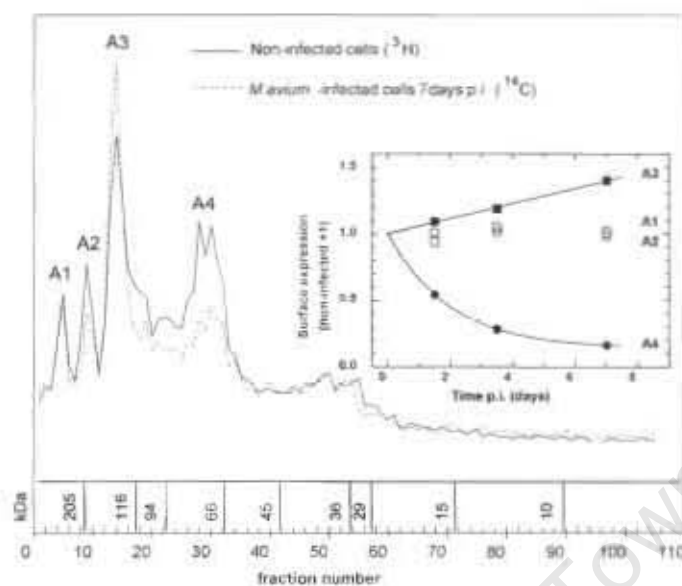


Figure 1. Changes in surface expression of integrin- α_M (peak A3) and integrin- β_2 (A4) on mouse bone marrow-derived macrophages in response to infection with *M. avium*. The main panel shows the SDS-PAGE profile of surface labelled glycoproteins of infected vs. non-infected cells (^{14}C vs. ^3H , resp.). The insert shows the post-infection (p.i.) time course of these changes. Modified from Itoe, B.Sc(med) Honours thesis, 2004.

1.3 The CR3 or Mac-1

1.3.1 Genes, biology, structure and functional domains

The genes for integrin $-\beta_2$ and $-\alpha_M$ subunits have been mapped to chromosomes 21 and 16 respectively (Marlin *et al.*, 1986). The β_2 protein has six N-linked extracellular glycosylation sites with a molecular weight of 95kDa. The alpha M chain has a molecular weight of 170kDa (Marlin *et al.*, 1986).

The $\alpha_M\beta_2$ complex, like the other β_2 integrin complexes, consists of a cytoplasmic tail, transmembrane, and N-terminal extracellular regions (see Diag. 2; Harris *et al.*, 2000).

The membrane-proximal cytoplasmic domain of the α_M chain contains a GFFKR motif. This motif serves as a “hinge” by forming a salt bridge with conserved residues on the β_2 chain, thus holding the α_M/β_2 heterodimer in a low-affinity conformation (Hughes *et al.*, 1996). The N-terminal extracellular region of the α_M subunit has 7 repeats that fold into a β -propeller structure (Springer, 1997). Inserted in the third repeat is a metal-ion (Mg^{2+} or Ca^{2+}) coordination site for ligand recognition. It contains approximately 200 amino acids. It is usually referred to as the I-domain or metal ion-dependent adhesion site (MIDAS) (Springer, 1997). The N-terminal extracellular region of the β_2 subunit contains an I-like domain of 241 amino acids analogous to I-domains of alpha subunits and also contains a MIDAS motif (shown as orange in diagram 2). The I-domain of alpha chains and the I-like domain of β_2 chain are required for interaction of $\alpha_M\beta_2$ with its ligand (Goodman and Bajt, 1996). These sites are overlapping but not identical (Zhang and Plow, 1996). The extracellular, membrane-proximal domains of both α_M and β_2 control the adhesive activity of CD11b/CD18. Site directed mutagenesis of these domains resulted in constitutive receptor activation (Xiong *et al.*, 2003).

Integrin- α_M and integrin- β_2 are present on the cell surface as a heterodimer, $\alpha_M\beta_2$ (CD11b/CD18), otherwise known as Mac-1 receptor or complement receptor type 3, CR3 (reviewed by Harris *et al.*, 2000). Mac-1 (membrane attack complex 1) or CR3 belongs to the integrin family of structurally related cell-surface receptors present on a wide range of cell types, especially leukocytes, where they play key roles in controlling important biological processes (Harris *et al.*, 2000). On the cell surface, integrins exist obligatorily as heterodimers composed of non-covalently associated α and β_2 subunits (Kürzinger and Springer, 1982). A common β_2 subunit can associate with one of four α subunits to form

different β_2 integrin receptors: $\alpha_L\beta_2$ (CD11a/CD18, LFA-1), $\alpha_M\beta_2$ (CD11b/CD18, Mac-1 or CR3), $\alpha_X\beta_2$ (CD11c/CD18, p150,95), $\alpha_D\beta_2$ (CD11d/CD18) [Sanchez-Madrid *et al.*, 1983].

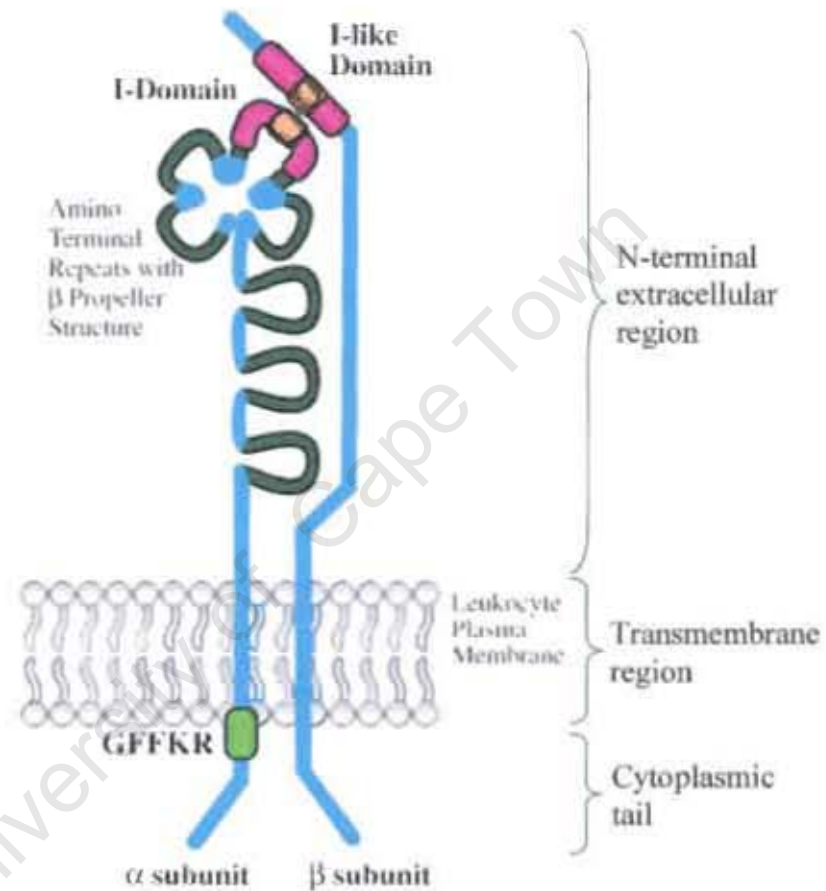


Diagram 2. **Features of β_2 integrins.** The α subunit has seven extracellular N-terminal homologous repeats organised into a β propeller structure. The I domain and the I-like domain of α and β subunits respectively, are indicated by pink with the MIDAS motif shown in orange. Reproduced from Harris *et al.*, 2000.

1.3.2 Role of CR3 in cell immunity

The CR3 receptor or Mac-1 plays key roles in immunity by mediating cell-cell contact through interaction with ICAM-1 and ICAM-2 on neighbouring cells, hence the term adhesion molecules (Diamond *et al.*, 1990). These adhesions result in homing of immune cells to sites of inflammation or infection (Grabbe *et al.*, 2002). An extensively studied function of Mac-1 as a complement receptor is its ability to bind to and remove C3bi-coated particles (Beller *et al.*, 1982; Wright *et al.*, 1983). C3bi is derived from the third component of complement, C3, as a result of cleavage of surface-bound C3b by serum enzyme I (Law *et al.*, 1979). CR3 also binds to the clotting factor fibrinogen (Altieri *et al.*, 1988) and the extracellular matrix protein fibronectin (Bohnsack and Zhou, 1992). Interactions between CR3 and its ligands C3bi and fibrinogen occur through distinct recognition domains present on CR3 (Wright *et al.*, 1983) and conserved Arg-Gly-Asp sequences present on C3bi and fibrinogen (Wright *et al.*, 1987).

Central to the elimination of invading pathogen is the process of phagocytosis. Uptake of pathogenic mycobacteria (Schlesinger, 1993; Bermudez *et al.*, 1999; Hu *et al.*, 2000; Rooyackers and Stokes, 2005) and *Bordetella pertussis* (Mobbeley-Schuman and Weiss, 2005) by macrophages can occur through CR3. This can either be opsonic or non-opsonic, depending on whether or not immunoglobulins (Igs) or complement factors are bound onto the surface of the bacteria (Allen *et al.*, 1996). CR3-mediated opsonic phagocytosis of mycobacteria occurs by interaction of the I-domain on CR3 with C3bi on the surface of the bacteria. Non-opsonic phagocytosis involves interaction of bacterial lipopolysaccharides with CR3 (Velasco *et al.*, 2003). Studies by Cywes *et al.* (1997) showed that non-opsonic phagocytosis of mycobacteria involves interaction of bacterial

lipopolysaccharides with beta glucan binding site on CR3 that is distinct from C3bi binding site. Le Cabec *et al.*, (2002) have demonstrated that under opsonic and non-opsonic conditions CR3 mediates type 1 and type 2 phagocytosis respectively.

Upon interaction with mycobacterial lipopolysaccharides, Mac-1 triggers intracellular signalling cascades that lead to diverse cellular behaviour such as cell migration (Ingalls and Golenlock, 1995; Reyes-Reyes *et al.*, 2002). In addition, Mac-1 also participates in the generation of a respiratory burst in synergy with Fc γ RIII (Zhou and Brown, 1994).

1.4 Thesis question

Regarding the pathogenicity of mycobacteria, what could be the role of reduced integrin- β_2 on the surface of infected macrophages? In an *in vivo* mouse infection model, and depending on the route of infection, it has been found that integrin- β_2 is down regulated on macrophages (Bonato *et al.*, 2001), but up-regulated on T- and B-lymphocytes (Bonato *et al.*, 2002). This could imply the absence of intercellular contact between infected macrophages and T- and B-lymphocytes and thus interfere with the release of cytokines for subsequent destruction of the infected cells.

This thesis was aimed at deciphering, under *in vitro* conditions, the mechanism(s) of integrin- β_2 down-regulation and concurrent up-regulation of integrin- α_M on the surface of mouse bone marrow-derived macrophages in response to mycobacterial infection and whether such changes can be brought about on non-infected macrophages by diffusible factors from infected macrophages. Furthermore, a reduced integrin- β_2 in the light of an enhanced surface expression of integrin- α_M raises the question of the identification of a possible alternative dimerization partner for integrin- α_M . The infection model for this

study is the same as previously used (B.Sc(med)Honours thesis, 2004). Bone marrow-derived macrophages from mice (C57BL6) were infected with *M. avium* (transparent colony variant TMC704, serovar, from the Trudeau Mycobacterial Culture Collection) to which the mice are susceptible both *in vivo* and *in vitro* (Frehel *et al.*, 1991). To measure the relative amounts of surface glycoproteins on infected against non-infected cells, these were surface-labelled enzymatically, with ^3H - galactose versus ^{14}C -galactose respectively (Thilo (1983), as depicted schematically in Diag. 3). The samples were mixed and compared in terms of their labelling profiles on a lane of SDS-PAGE. By combining immunofluorescence, Western blotting, real time reverse transcription polymerase chain reaction (RT-PCR), together with exogalactosylation, we report that the changes in integrin surface-expression were not based on changes at the transcriptional level. Therefore, infection of macrophages with *M. avium* caused a redistribution of integrin- α_M and - β_2 between intracellular and plasma-membrane pools. Also, diffusible factors in the medium from infected cells caused a similar altered surface expression of integrin- α_M and - β_2 on non-infected macrophages. Because surface expression of integrins occurs obligatory in pairs in the form of heterodimers, the alternative substituting dimerization partner of the enhanced integrin- α_M was investigated by subjecting lysates from *M. avium*-infected and non-infected cells to co-immunoprecipitation with an anti-integrin- α_M antibody. The analysis showed no additional dimerisation partner for integrin- α_M to complement the reduction of surface integrin- β_2 .

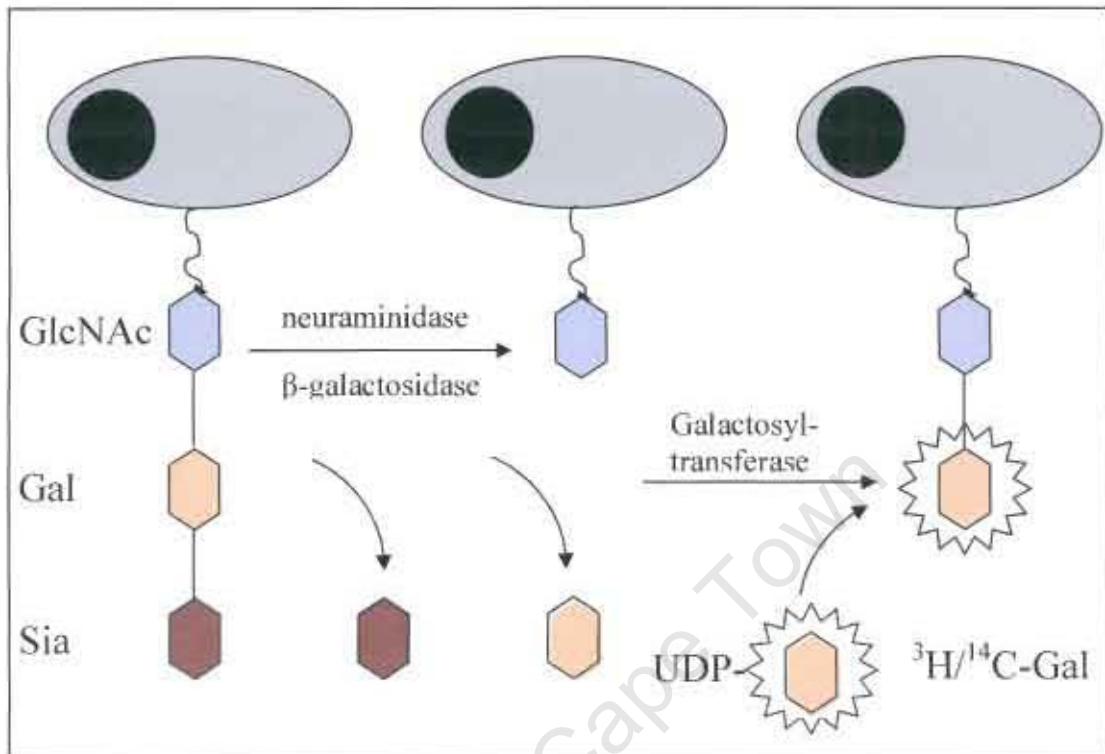


Diagram 3. **Schematic representation of radiolabelling of cell-surface glycoproteins.** Pre-treatment of cells with β -galactosidase removes galactose and sialic acid residues from sugar side-chains. Addition of ^3H -galactose or ^{14}C -galactose is catalyzed by galactosyl-transferase. Adapted from Thilo, 1983.

Chapter 2: RESULTS

2.1 Optimisation of methods

Infection of mouse bone marrow-derived macrophages with *M. avium* caused an altered surface expression of radiolabelled glycoconjugates, particularly integrin- α_M and integrin- β_2 (Itoe, B.Sc(med)Honours degree, 2004). In order to study the underlying mechanism, several methods had to be developed for making semi-quantitative observations for integrin- α_M and integrin- β_2 expression. These were: immunofluorescence, Western blotting, reverse transcription polymerase chain reaction (RT-PCR). In addition, the possibility of co-immunoprecipitating integrin- α_M with its possible dimerisation partner was also tested and examined in the context of reduced surface expression of integrin- β_2 .

2.1.1 Immunofluorescence for comparing cell-surface integrins

2.1.1.1 Optimisation of antibody dilutions

In order to find suitable dilutions of anti-integrin- β_2 or anti-integrin- α_M antibody for immunofluorescence, mouse bone marrows derived macrophages, cultured on a film of Petriperm, were stained with different dilutions (1/100 and 1/500) of either FITC-conjugated anti-integrin- β_2 monoclonal antibody C71/16 or Alexa 488-conjugated anti-integrin- α_M monoclonal antibody M1/70. The nuclei were stained with DAPI. A suitably intense staining was obtained for both antibodies at an antibody dilution of 1/100, as shown in Fig. 2 for the anti-integrin- β_2 antibody.

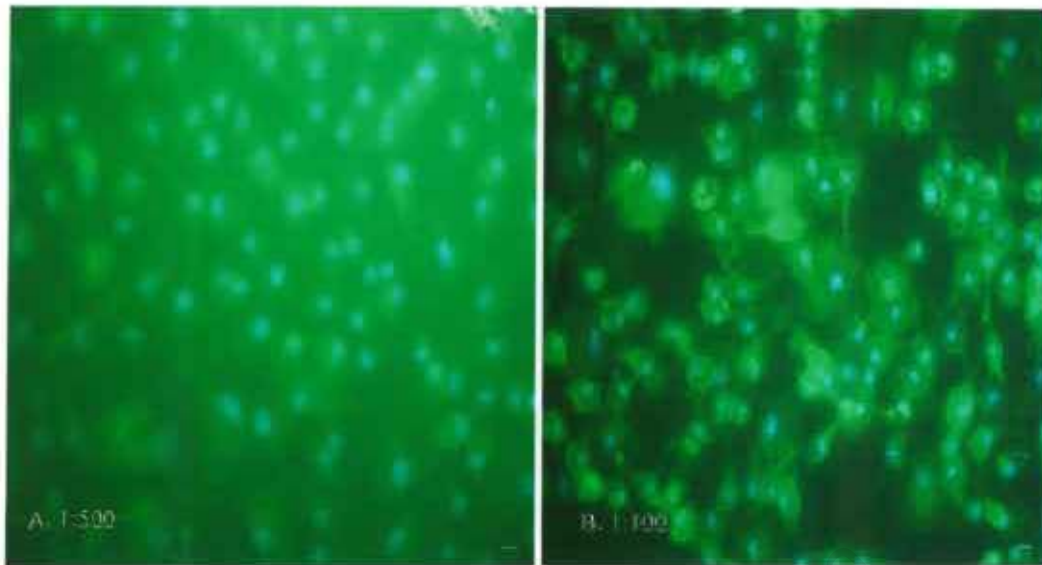


Figure 2. **Staining with different dilutions of anti-integrin- β_2 antibody.** Macrophages were cultured on Petriperm over 14days and stained with antibody dilution of 1:500 (A) or 1:100 (B). Antibody staining shows up as green. Blue indicates DAPI-stained nuclei. Suitably intense staining was obtained for a dilution of 1: 100. The scale bar represents 4 μ m.

2.1.1.2 Specificity of staining with anti-integrin- α_M antibody M1/70

To determine the specificity of surface staining for integrin- α_M , macrophages were first stained with unconjugated purified rat anti-mouse anti-integrin- α_M antibody [M1/70] at 1/100 dilution followed by incubation with Alexa 488-conjugated M1/70 at the same dilution. The nuclei were stained with DAPI. As shown in Fig. 3, no non-specific green fluorescence was observed after blocking with unconjugated antibody. The specificity of staining with anti-integrin- β_2 antibody C71/16 was not measured.

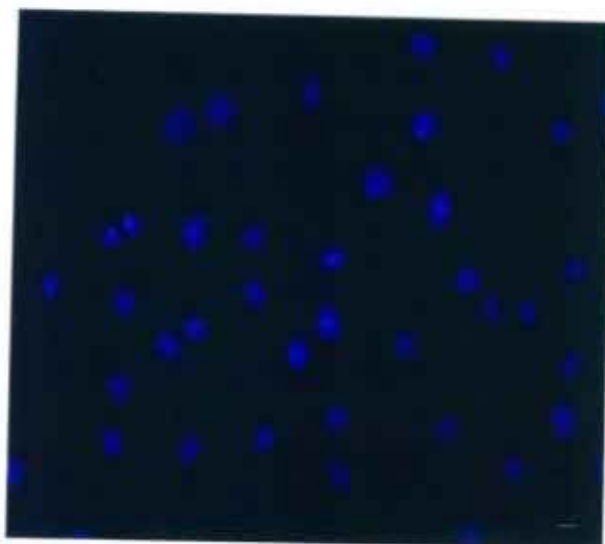


Figure 3. **Specificity of staining with Alexa 488-conjugated anti-integrin- α_M antibody M1/70.** Macrophages were first stained with unconjugated M1/70 and then with Alexa 488-conjugated M1/70. Blue indicates nuclei that were stained with DAPI. Surface staining was abolished by blocking with unconjugated antibody. The size bar represents 3 μm .

2.1.2 Western blot conditions for semi-quantitative detection

2.1.2.1 Dilution of anti-integrin- β_2 antibody C71/16

In order to determine the concentration of anti-integrin- β_2 antibody and the amount of protein suitable for quantitative Western blotting, four sets each of 2 μg , 4 μg , 8 μg , and 16 μg of proteins were analyzed on an 8% SDS-PAGE and transferred onto a nitrocellulose membrane. Sections of the nitrocellulose membrane, each with a single set of proteins, were incubated in different dilutions of anti-integrin- β_2 monoclonal antibody C71/16 [(I) 1/200, (II) 1/1000, (III) 1/5000, (IV) 1/10000], but in the same dilution (1/1000) of secondary HRP-conjugated antibody NA935V. Fig. 4B shows densitometry

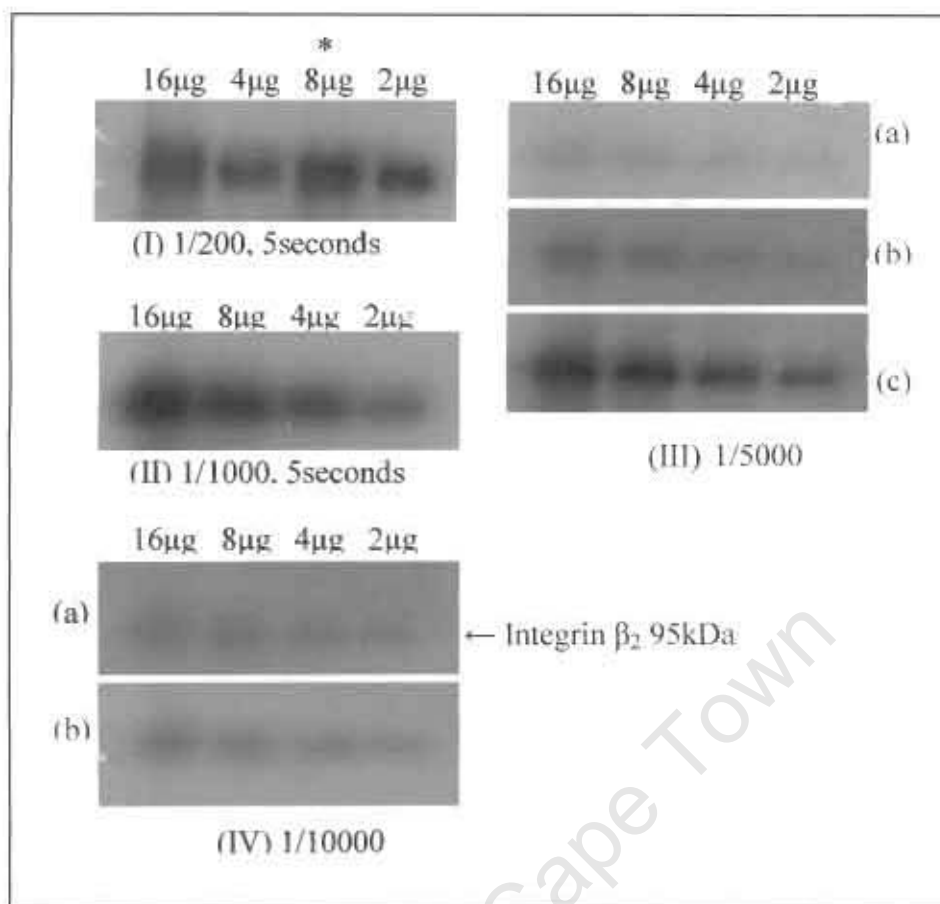


Figure 4A. **Optimisation of Western blot conditions for anti-integrin β_2 antibody.** Doubling amounts of membrane protein from uninfected macrophages were analysed on an 8% SDS-PAGE under non-denaturing conditions and subjected to Western blotting using different dilutions of anti-integrin- β_2 antibody, but the same 1/1000 dilution of HRP-conjugated antibody. (I) 1/200 dilution of anti-integrin- β_2 antibody, 5 seconds exposure, (II) 1/1000 dilution, 5 seconds exposure, (III) 1/5000 dilution, exposed (a) 5 seconds (b) 10seconds (c) 15seconds and (IV) 1/10000 dilution, exposed (a) 15seconds (b) 30seconds. Densitometric scans are shown in fig. 4B. * Inverted loading.

analyses of bands in Fig. 4A. The signal was approximately linear at a dilution of anti-integrin- β_2 antibody of either 1/10000 with an exposure of 15-30 seconds (panel IV) or 1/5000 with an exposure of 10-15seconds (panels III b, c), and a protein amount of 2 μ g or 4 μ g (Fig. 4B). All subsequent Western blotting with anti-integrin- β_2 antibody C71/16 was done at a dilution of 1/10000 and a protein amount of 2 μ g or 4 μ g.

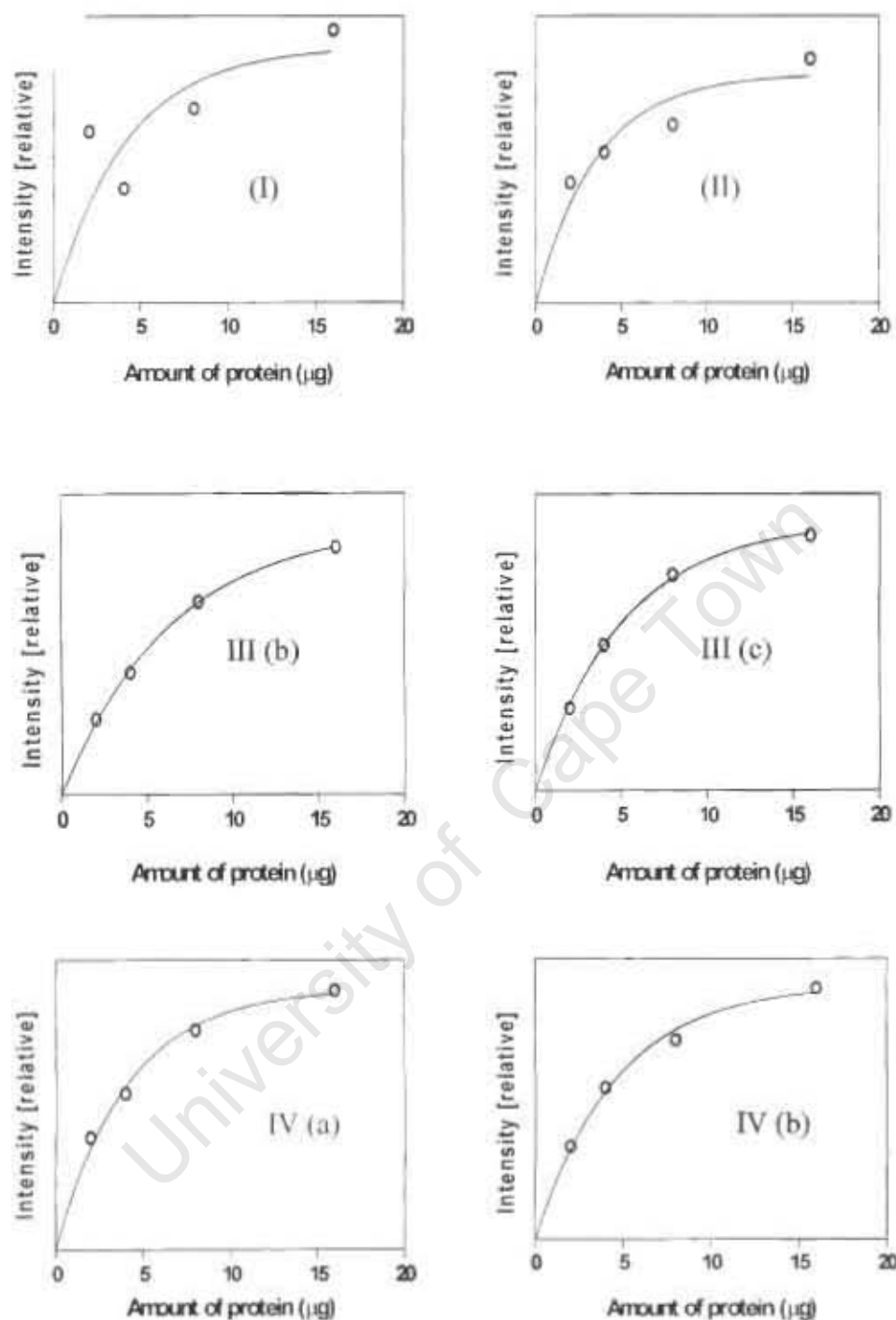


Figure 4B. Densitometric analyses for optimization of anti-integrin- β_2 antibody dilutions in Western blots. Doubling amounts of membrane proteins were analysed on an 8% SDS-PAGE under non-denaturing conditions and subjected to Western blotting as in Fig. 4A. The intensities of the bands obtained at different antibody dilutions were scanned with a densitometer to obtain integrated peak values. The plots I, II, III (b), III (c), IV (a), and IV (b) were obtained from the corresponding blots shown in Fig. 4A. No such analysis was done for III (a) because the signal was close to background.

2.1.2.2 Dilution of anti-integrin- α_M polyclonal antibody M-19

Similarly, as in section 2.1.2.1, sets of membrane proteins were prepared from mouse macrophages and analysed on SDS-PAGE, followed by Western blotting. The antibody M1/70 as used for immunostaining in section 2.1.1 was tested and no signal was detected for staining of Western blots. Another anti-integrin- α_M antibody, M-19, was obtained and tested for detection of integrin- α_M on Western blots. To determine the dilution of goat anti-integrin- α_M polyclonal antibody M-19, and the amount of protein to be used for Western blotting of integrin- α_M antigen, sections of nitrocellulose membrane containing a single set of protein were incubated in different dilutions of antibody, followed by incubation in the same dilution (1/1000) of secondary HRP-conjugated rat anti-goat antibody. In addition, the concentration of secondary antibody was varied. Sections of nitrocellulose membrane containing a single set of protein were first incubated in the same dilution of anti-integrin- α_M antibody (1/200) but different dilutions of secondary antibody. As observed in Fig. 5 (I) a, b, and (II) a, a faint band for integrin- α_M masked by non-specific background could be detected only when the nitrocellulose membrane was incubated in anti-integrin- α_M antibody dilutions of 1/100 and 1/200, using a secondary antibody dilution of 1/1000. Due to the presence of non-specific background that overwhelmed the detection of integrin- α_M band, Western blot experiments comparing relative expression of integrin- α_M antigen could not be performed using this antibody. No other antibodies were commercially available for this purpose.

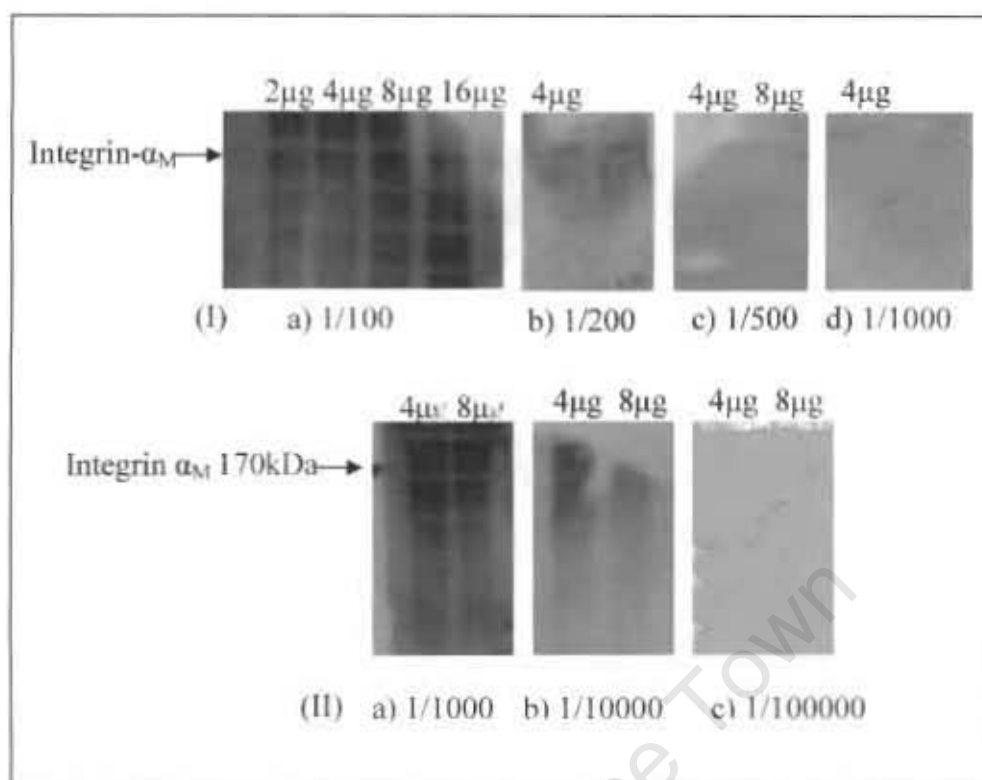


Figure 5. **Western blot conditions for anti-integrin- α_M polyclonal antibody M-19.** Sets of plasma membrane proteins were analysed on an 8% SDS-PAGE and subjected to Western blotting using either different dilutions of primary anti-integrin- α_M polyclonal antibody [(I) a) 1/100, b) 1/200, c) 1/500, and d) 1/1000] but the same dilution (1/1000) of secondary anti-goat HRP-conjugated antibody, or the same dilution (1/200) of primary antibody but different concentration of secondary antibody [(II) a) 1/1000, b) 1/10000, and c) 1/100000].

2.1.3 RT-PCR conditions for measuring integrin gene expression

2.1.3.1 Quality of isolated RNA

RNA was isolated from *M. avium*-infected and uninfected macrophages by the Trizol RNA isolation method as described in Materials and Methods. To determine the quality of isolated RNA, 2 μ g and 4 μ g of RNA were electrophoresed in a 1.5% formaldehyde agarose gel. Three distinct bands were observed, representing 28, 18 and 5 subunits of

ribosomal RNA (Fig. 6). This indicated that the RNA was of good quality to be used for cDNA synthesis.

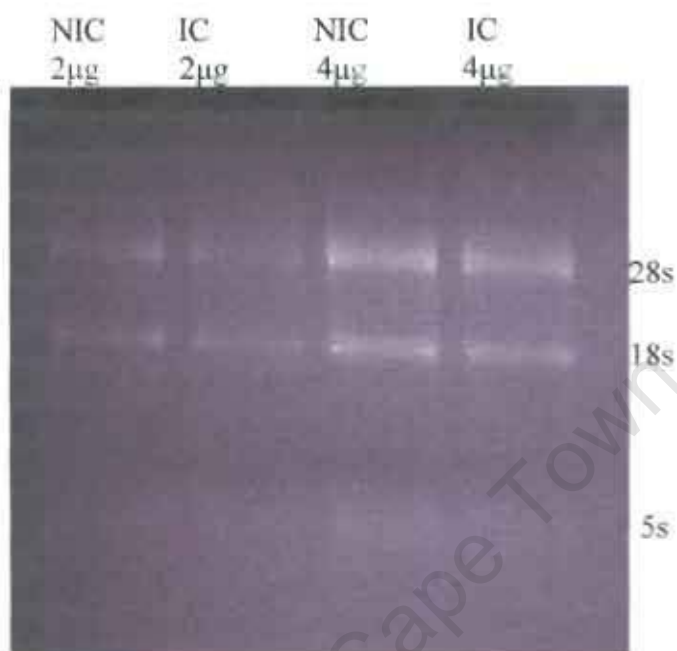


Figure 6. **Quality of RNA isolated from *M. avium*-infected and uninfected mouse bone marrow-derived macrophages.** After 7days of infection (IC) with *M. avium* or not (NIC), RNA was isolated from mouse bone marrow-derived macrophages by the Trizol RNA isolation method as described in Materials and Method, and analysed on a 1.5% formaldehyde agarose gel. The ethidium bromide-stained bands represent the 28, 18 and 5 subunits of ribosomal RNA.

2.1.3.2 Specificity of designed primers

Pairs of primers were synthesized to cross the exon-intron boundaries for exon 5 of the integrin- β_2 gene and exon 29 of the integrin- α_M gene, as described in Materials and Methods. To test the specificity of these primers for amplification, cDNA was prepared as described in the Materials and Methods and amplified by the polymerase chain reaction (PCR). As a control, the cDNA for Glyceraldehyde-3-phosphate dehydrogenase

(GAPDH) was amplified as a housekeeping gene. The PCR products were analyzed on an agarose gel and the specificity of the primers for amplification of these genes was confirmed by the appearance of a single band corresponding to the right molecular weight for each exon amplified (Fig. 7): integrin α_M -140 basepairs(bp); integrin β_2 -170 basepairs (bp); GAPDH -192 basepairs (bp).

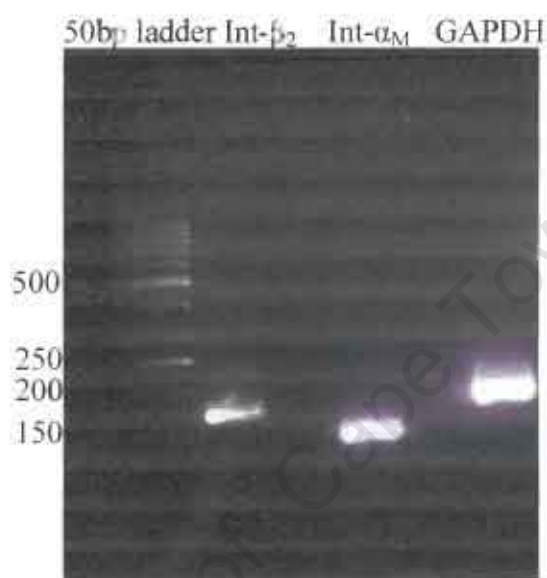


Figure 7. Analysis of test PCR products on 2% agarose gel. cDNA was prepared from macrophages and amplified by polymerase chain reaction (PCR) using primers specific to integrin- β_2 (170bp), integrin- α_M (140bp) and GAPDH (192bp, as control) genes. The PCR products were analysed on a 2% ethidium bromide-stained agarose gel.

2.1.4 Determination of optimal cell count needed for co-immunoprecipitation of integrin- β_2 with - α_M

Integrin- α_M and integrin- β_2 obligatorily occur as a heterodimer (known as Mac-1 or CD11b/CD18) on the cell-surface of macrophages and neutrophils. P388D1 is a murine macrophage cell line that is readily available in our laboratory. The expression of integrin- β_2 and integrin- α_M on P388D1 cells was previously confirmed either by

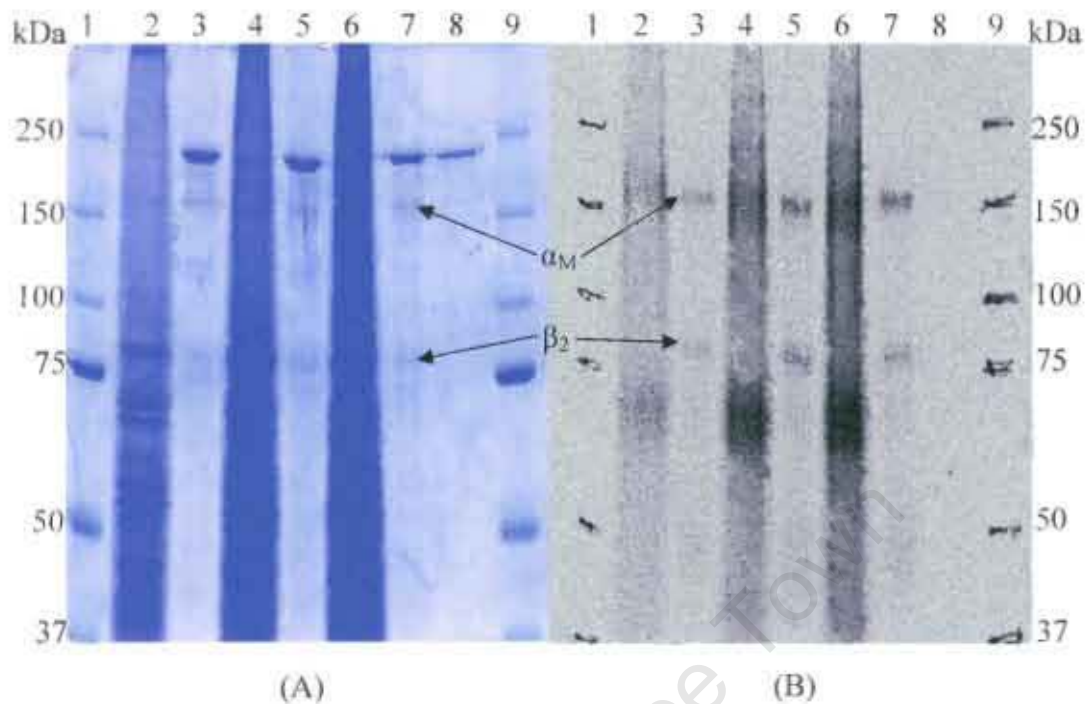


Figure 8. **Co-immunoprecipitation of ^{14}C -surface-labelled $\alpha_{\text{M}}\beta_2$.** P388D1 murine macrophages were radioactively surface-labelled with ^{14}C -galactose, lysed, and proteins subjected to co-immunoprecipitation using rat anti-integrin α_{M} monoclonal antibody. The ^{14}C -labelled membrane protein supernatants and immunoprecipitates from 5×10^6 (lanes 2 and 3), 10×10^6 (lanes 4 and 5) and 15×10^6 (lanes 6 and 7) cells were analysed on 7% SDS-PAGE under non-denaturing conditions. A: Coomassie-stained gel, B: autoradiogram. Lane 8 contained non-denatured antibody. Lanes 1 and 9 are contained precision stain molecular-weight markers (in B, markers were traced with ^{14}C -labelled ink).

immunostaining with FITC-conjugated anti-integrin- β_2 and Alexa 488-conjugated integrin- α_{M} or immunoblotting with anti-integrin- β_2 antibody. To determine the number of cells necessary for co-immunoprecipitation of integrin- β_2 enough for detection by Coomassie Brilliant Blue-staining and by autoradiography, 5×10^6 , 10×10^6 , and 15×10^6 cells were surface-labelled with ^{14}C -galactose, lysed, and incubated with a fixed amount of anti-integrin- α_{M} monoclonal antibody M1/70 ($20 \mu\text{g}$) as described in Materials and

Methods. The immunoprecipitates and supernatants from each cell count were analyzed on SDS-PAGE and the presence of either integrin- α_M or integrin- β_2 was confirmed by Coomassie-blue staining followed by autoradiography as shown in Fig. 8. Similar and easily detectable bands corresponding to integrin- α_M and integrin- β_2 can be obtained from a cell count of either 10×10^6 or 15×10^6 , Fig. 8(B).

2.2 Results

2.2.1 Macrophages contained actively replicating and viable bacteria

Following optimization of methods, it was important to confirm whether the infection of macrophages with *M. avium* was successful. Seven days old *M. avium*-infected cells were fixed with 2.5% glutaraldehyde, followed by 1% OsO₄ and then

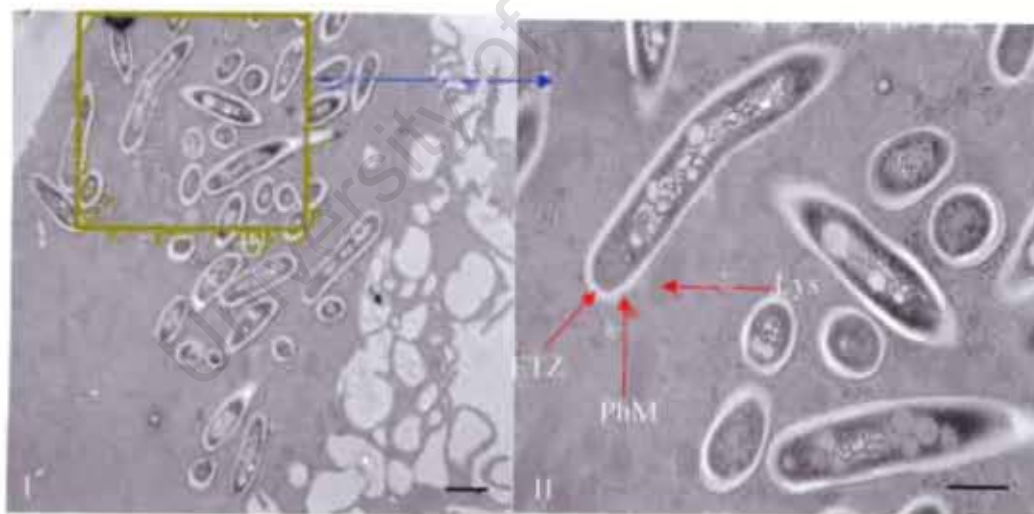


Figure 9. **Thin sections of *M. avium*-infected mouse bone marrow-derived macrophages.** At 7days post-infection, *M.avium*-infected cells were fixed for electron microscopy as described in Materials and Methods. Panel II is an enlarged portion of the box in section I. (ETZ) indicates an electron translucent layer of the mycobacterial cell wall. (PhM) indicates phagosome membrane. (Ly) indicates a lysosome. The size bar for section I is 1 μ m and that of section II is 0.5 μ m. (Courtesy of Dr. C. de Chastellier).

processed for electron microscopy observation as shown in Fig. 9. The cells and the bacteria are ultrastructurally intact and the latter are located in separate phagosomes. No evidence of phagosome-lysosome fusion could be seen in all the sections viewed.

2.2.2 Labelling of plasma-membrane glycoconjugates

The present analyses are based on our previous observation that infection of macrophages with *M. avium* caused an increased and a decreased surface expression of integrin- α_M and integrin- β_2 , respectively (Itoe, B.Sc(med)Honours thesis, 2004). To confirm this, cell-surface glycoconjugates were labelled with radioactive galactose and then subjected to SDS-PAGE and trypsin ingel digestion analyses. To obtain labelled plasma-membrane glycoproteins from *M. avium*-infected and non-infected mouse bone marrow-derived macrophages, fractions from both sets of cells were labelled enzymatically with ^{14}C -galactose and ^3H -galactose in the presence of galactosyltransferase at 4°C , as shown schematically in Diag. 3 (Thilo, 1983). The four sets of cells were homogenized separately and postnuclear supernatants were prepared. These were centrifuged separately on self-forming 27% Percoll density gradients to remove high-density lysosomes (bottom of gradient) and cytosolic proteins (overlay volume) as described in Materials and Methods. ^{14}C - and ^3H -labelled glycoproteins were restricted to the top of the gradient as in Fig. 10. Plasma membrane glycoproteins together with other intracellular organelles such as endosomes, endoplasmic recticulum and golgi apparatus are less dense than lysosomes and sediment at the top of the column after centrifugation. (Merion and Sly, 1983).

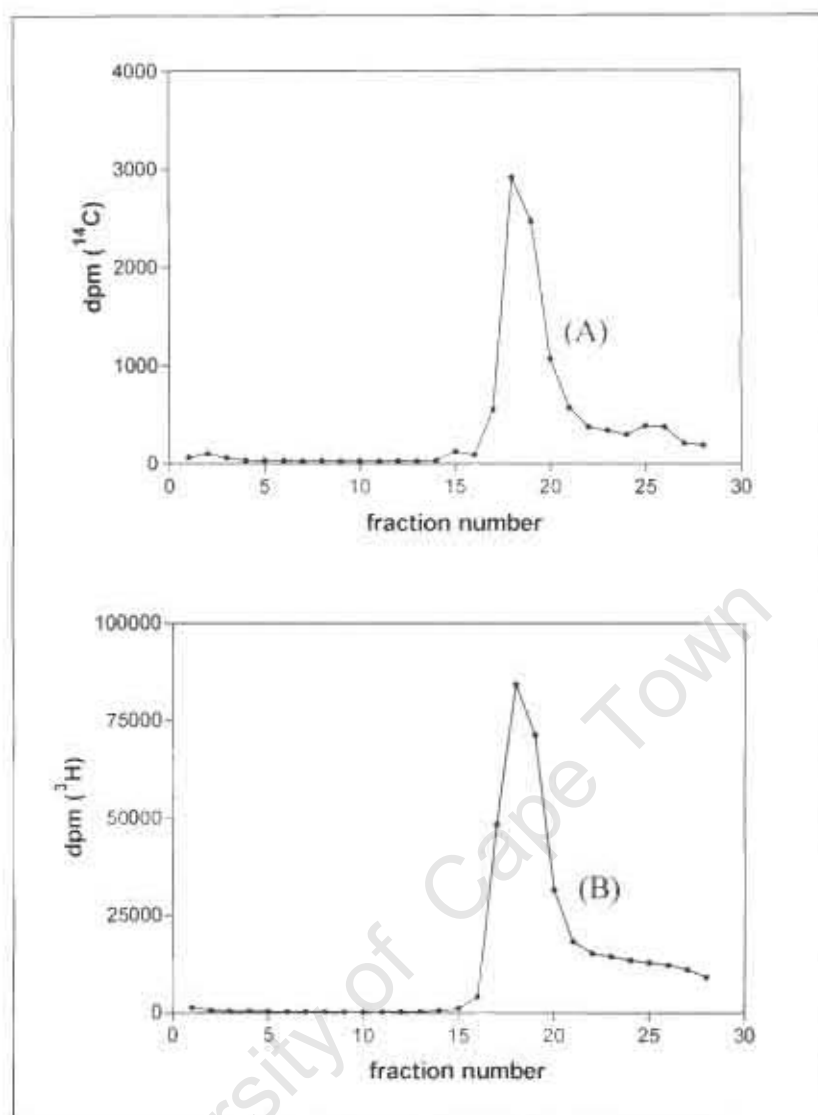


Figure 10. **Partitioning of labelled plasma-membrane glycoprotein by density centrifugation on 27% Percoll gradients.** Macrophages were infected (IC) or not (NIC) with *M. avium*. At 7 days post-infection, surface glycoconjugates were labelled with ^{14}C -galactose (A) and ^3H -galactose (B) respectively, as described in Materials and Methods. Post-nuclear supernatants (PNS) were prepared, layered on separate 27% Percoll density gradients and centrifuged. Fractions of 0.5ml were collected from the bottom. An aliquot of 20 μl was taken from each fraction and counted in a liquid scintillation counter. The amount of label (dpm) was plotted against fraction number. Fractions 17-20 contained labelled membranes. Overlay volume was contained in fractions 21 to 28.

2.2.3 SDS-PAGE of ^{14}C -labelled plasma membrane

To compare plasma-membrane glycoproteins from *M. avium*-infected and non-infected mouse bone marrow-derived macrophages, a mixture of ^{14}C -labelled and ^3H -labelled plasma-membrane proteins from both cell types was analysed on an 8%-15% gradient SDS-PAGE under denaturing conditions and the gel was Coomassie-stained [Fig. 11(I)]. The distribution of ^{14}C -labelled membrane from *M. avium*-infected cells was obtained by exposing the gel to a cyclone phosphor imager. Four prominent bands can be seen on the autoradiogram [Fig. 11(II)]. ^3H -label is not detected.

University of Cape Town

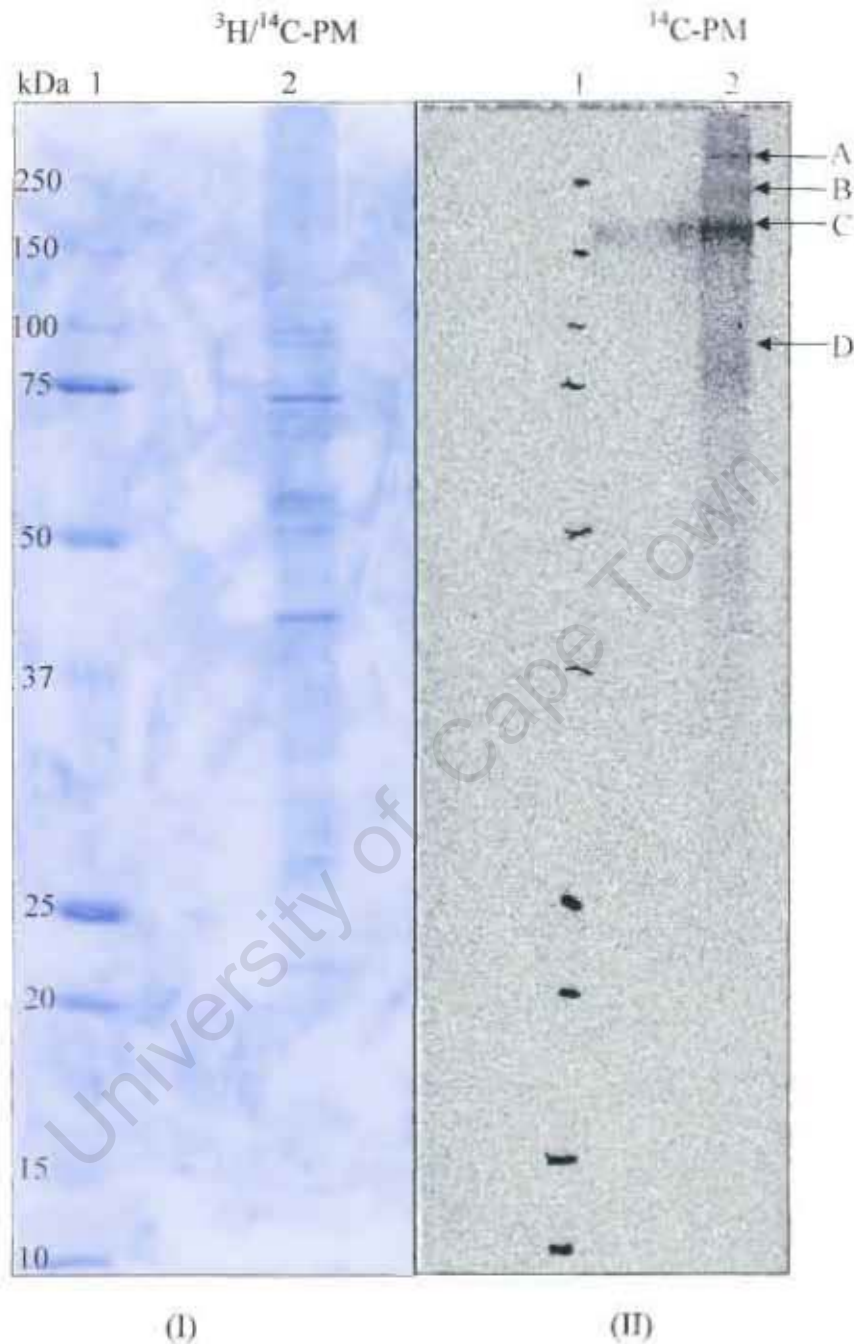


Figure 11. SDS-PAGE of membrane proteins. ^{14}C - and ^3H -labelled membrane proteins were isolated from *M. avium*-infected (7 days post-infection) and uninfected macrophages respectively. The membranes were mixed and analysed on the same lane of an 8%-15% gradient SDS-PAGE. (I): Coomassie-stained gel, (II): autoradiogram. Lane 1 contained precision stain marker which was traced with ^{14}C -labelled ink for autoradiography (as in II). Lane 2 contained mixed ^{14}C - and ^3H -labelled membrane samples.

2.2.4 Trypsin ingel digestion for ^{14}C - and ^3H -labelled plasma membrane

Because beta emission from ^3H has too low energy for detection by autoradiogram, lane 2 in Fig. 11(I) was subsequently subjected to trypsin digestion as described in Materials and Methods in order to release labeled protein fragments. The digestion products were plotted against fraction number. In order to obtain a direct comparison between ^{14}C - and ^3H -labelled plasma-membrane proteins from *M. avium*-infected and uninfected macrophages, respectively, the profiles were normalized so as to obtain the same area under each curve. As we have previously shown, there was a decreased expression on *M. avium*-infected cells of ^{14}C -labelled membrane glycoproteins in the 70-100kDa region and an increased expression of glycoproteins in the 100kDa. (Fig.12). MALDI-TOF analysis showed that the most obvious changes were observed for integrin- β_2 and integrin- α_M , with integrin- β_2 being down-regulated and integrin- α_M being up-regulated (Itoe, B.Sc(med)Honours thesis, 2004).

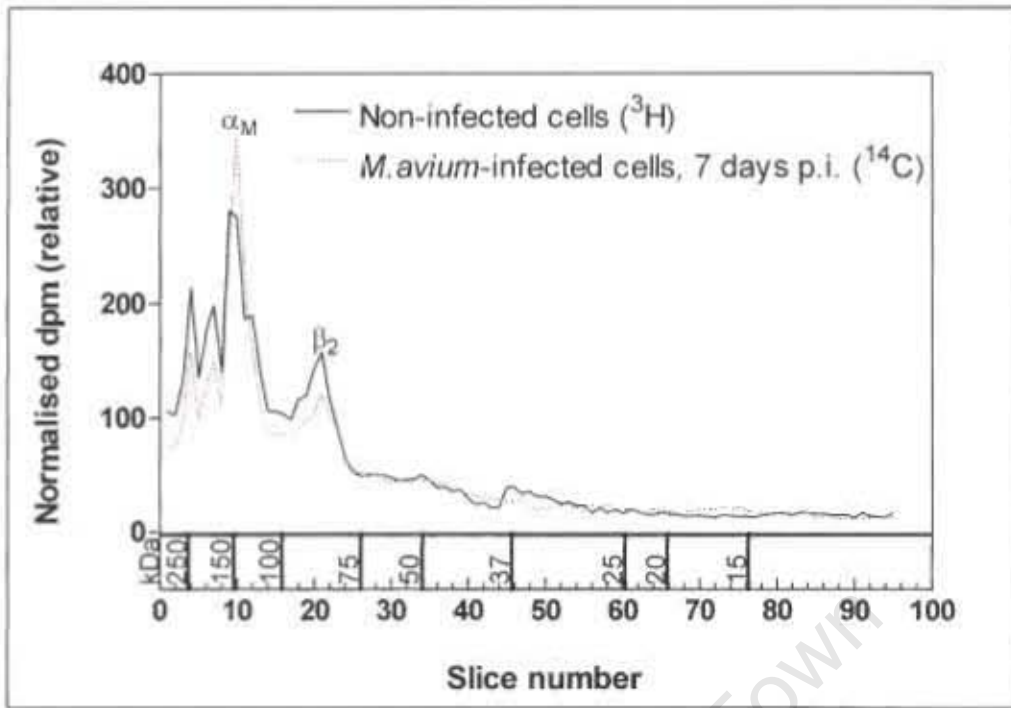


Figure 12. **Differential cell-surface expression of glycoproteins on *M. avium*-infected (7days post-infection) and non-infected macrophages.** A mixture of ^{14}C and ^3H -labelled plasma membrane from infected and non-infected mouse bone marrow-derived macrophages, respectively, was analyzed on an 8%-15% gradient SDS-PAGE as in Fig. 11(I). Lane 2 was cut into 2.5mm wide slices that were then trypsinized as described in Materials and Methods in order to release labelled protein fragments. The label from each slice was counted twice in a liquid-scintillation counter and an average taken. The amount of dpm from each slice was plotted against slice number. Because the total counts for ^3H and ^{14}C were different, the profiles as shown were normalized such that the total areas under the curves were the same. A down-regulation of cell-surface labelled glycoproteins on infected cells was observed in the 75-100kDa region. An up-regulation of labelled glycoproteins was observed in the 150-200 kDa region.

2.2.5 Does the decrease in integrin- β_2 occur at a transcriptional or translational level?

To determine if the decrease observed for radiolabelled integrin- β_2 protein as shown in Fig. 12 were occurring at the translational or at the transcription level, total membrane proteins from infected and non-infected macrophages were prepared as described in the

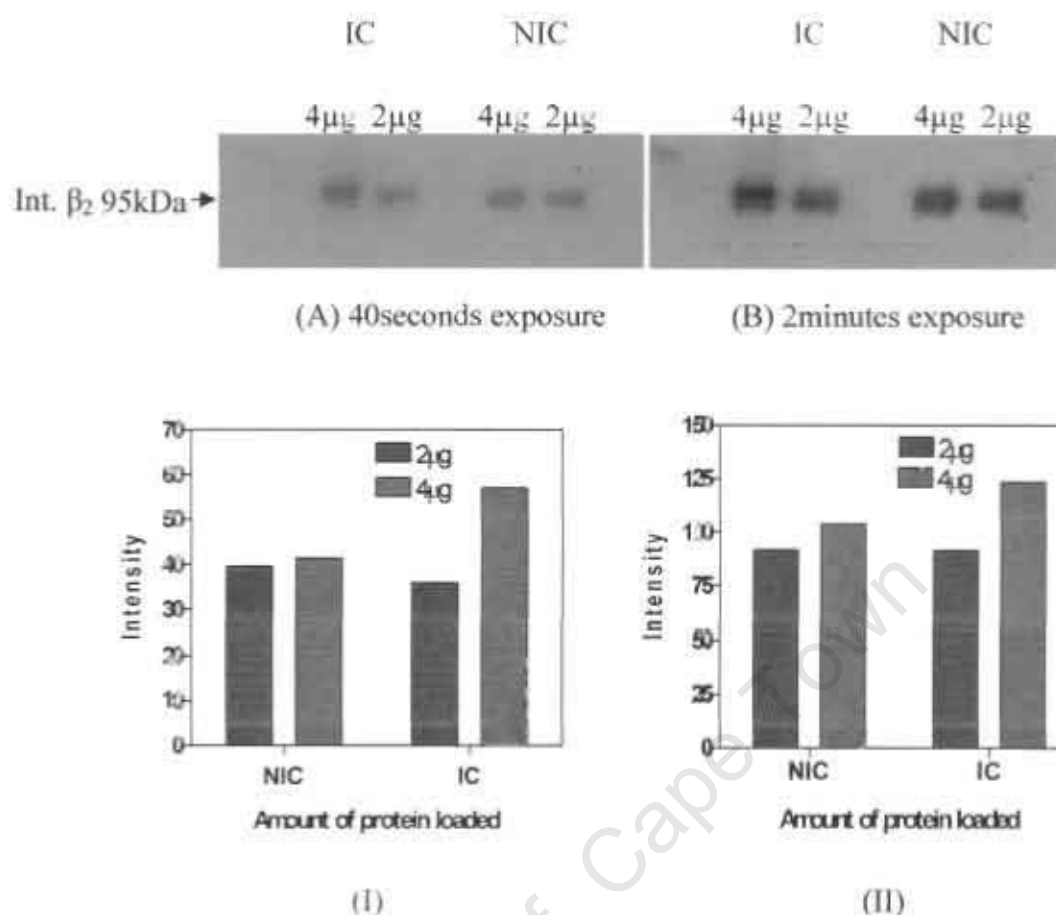


Figure 13. Comparative expression of integrin- β_2 in macrophages, with or without infection with *M. avium*. Seven days post-infection, doubled amounts of total membrane proteins (2 μ g and 4 μ g per lane) from infected cells (IC) and non-infected cells (NIC) were analysed by Western blotting from 8% SDS-PAGE, using anti-integrin β_2 antibody (C71/16). The intensities of the bands were determined using a densitometer.

Materials and Methods. The membrane proteins were sonicated in high salt to remove luminal enzymes. Previously determined suitable amounts of 2 μ g and 4 μ g of total membrane protein (section 2.1.2) from each sample were analyzed by Western blotting from an 8% SDS-PAGE using rat anti-integrin- β_2 monoclonal antibody (C71/16) as in Fig. 13 A and B. The relative intensities of the bands, analysed by densitometry, were as

in Fig. 13(I) and 13(II). No significant difference was observed for the relative amount of integrin β_2 on total membrane protein from *M. avium*-infected (IC) and non-infected cells (NIC). This suggested that the decreased and increased cell-surface expression of integrin- β_2 and integrin- α_M , respectively, observed on *M. avium*-infected macrophages was not due to changes at the level of protein synthesis. To confirm the results obtained in Fig. 13, relative gene expression of integrin- α_M and integrin- β_2 genes was determined by quantitative real-time PCR using primers spanning the intron-exon boundaries for exon 5 of the integrin- β_2 gene and exon 29 of the integrin- α_M gene. No significant difference was observed for integrin- α_M and - β_2 gene expression between *M. avium*-infected and uninfected macrophages as shown in Fig. 14. GAPDH was used as a control housekeeping gene in both cases. The specificity of amplification was checked by analyzing the PCR products on an ethidium bromide-stained 2% agarose gel as shown in Fig. 15. Only single bands were observed and no primer dimers.

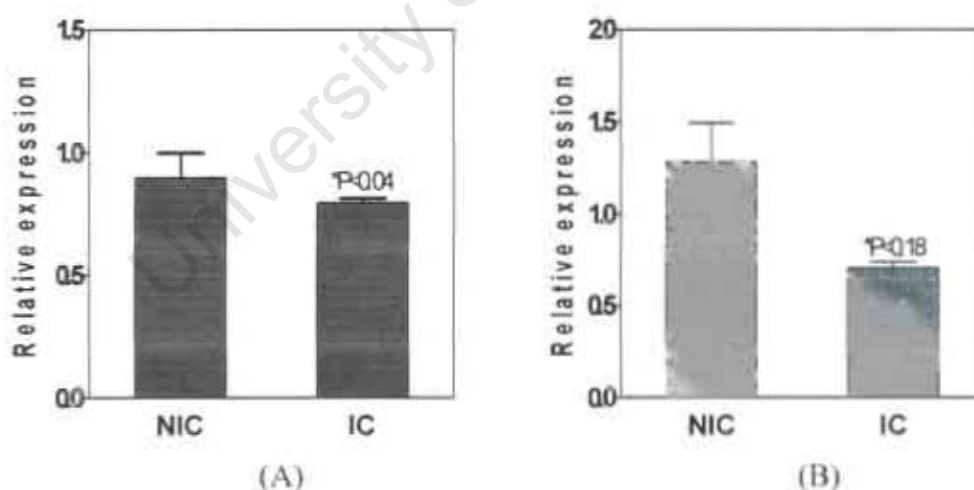


Figure 14. Expression of integrin- β_2 and - α_M genes of mouse bone marrow-derived macrophages upon infection with or without *M. avium*. cDNA was prepared from non-infected (NIC) and *M. avium*-infected (IC) mouse bone marrow-derived macrophages at day 7 after infection and amplified using pairs of specific primers. (A) expression of integrin- β_2 gene, with $P < 0.04$ and (B) expression of integrin- α_M gene, with $P < 0.18$. Results are from a single experiment performed in triplicate.

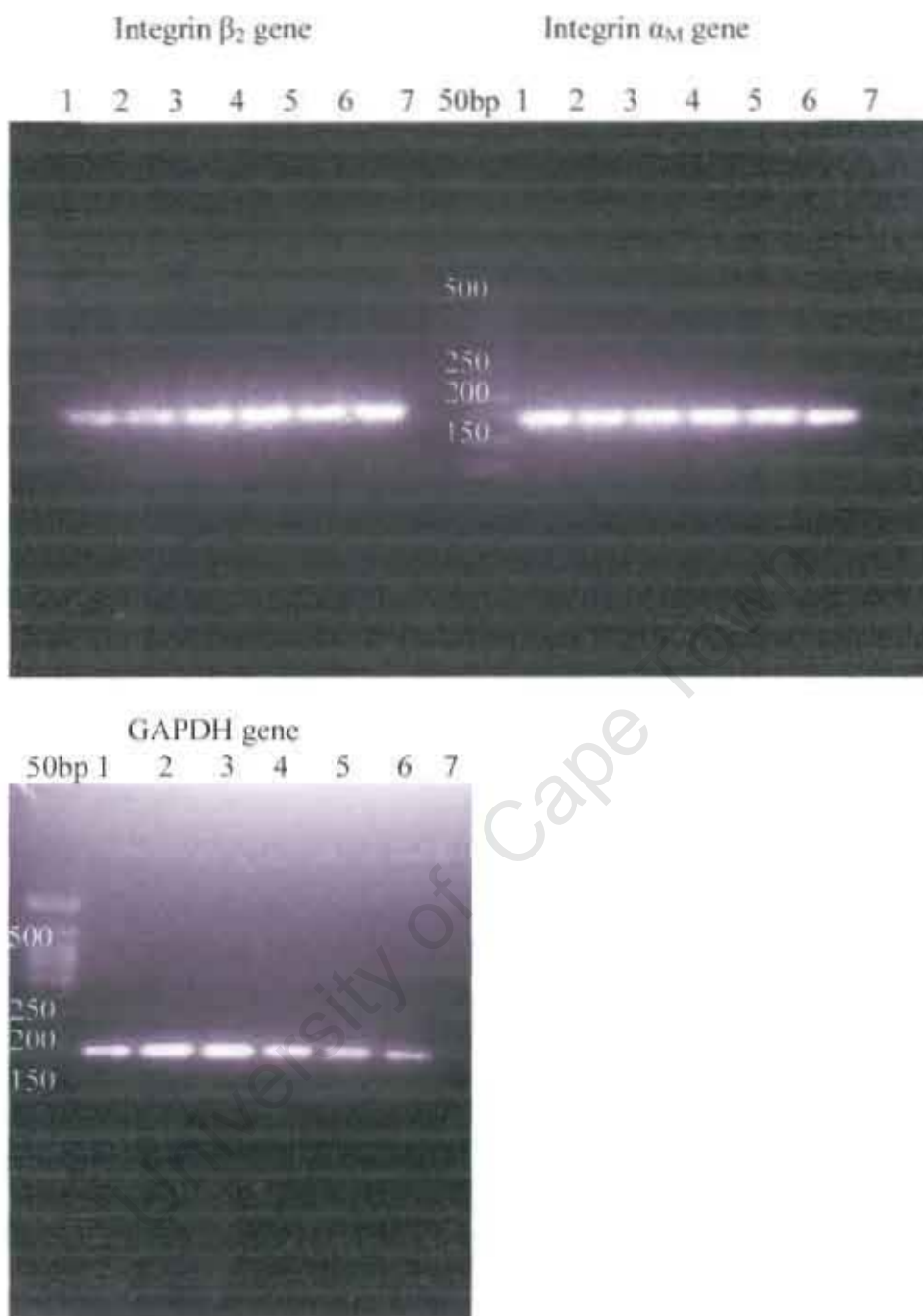


Figure 15. Polymerase chain reaction amplification of integrin α_M and β_2 from *M. avium*-infected and non-infected mouse bone marrow-derived macrophages. At day 7 after infection, cDNA was prepared from *M. avium*-infected and non-infected mouse bone marrow-derived macrophages and amplified for integrin α_M , integrin β_2 , and GAPDH genes using pairs of specific primers. The PCR products were analysed on a 2% agarose gel and photographed. In lanes 1, 2, and 3, cDNA from *M. avium*-infected cells was used. Lanes 4, 5, and 6, cDNA from non-infected cells was used. In lane 7, H₂O was used as a control.

2.2.6 Differential surface expression of integrin- α_M and integrin- β_2 on macrophages in response to infection with *M. avium*

Analysis by Western blotting showed no significant differences in the amount of integrin- β_2 on total membrane protein from infected and non-infected macrophages (Fig. 13). To confirm if the changes observed for radiolabelled plasma-membrane proteins from *M. avium*-infected cells (Fig. 12) denote an overall change in total protein pool, *M. avium*-infected and non-infected mouse bone marrow-derived macrophages were separately subjected to surface immunolabelling with either Alexa 488-conjugated anti-integrin- α_M monoclonal antibody M1/70 or FITC-conjugated anti-integrin- β_2 monoclonal antibody (C71/16). The nuclei were stained with DAPI. The images (Fig. 16 and Fig. 17) were normalized for brightness by using the same exposure time for both test and control samples. When these images were analysed for relative intensity of fluorescence signal, no significant difference was obtained between infected and non-infected cells (Fig. 18). The corresponding numbers for integrin- β_2 for non-infected and infected cells were 530 ± 19.1 and 557.6 ± 19.1 respectively ($P < 0.02$). For integrin- α_M , the values were 445.7 ± 49.5 and 515 ± 49.5 ($P < 0.05$) for non-infected and infected cells respectively. The surface staining procedure appeared to be insufficiently sensitive for detecting the decreased or increased surface expression of integrin- β_2 or integrin- α_M respectively.

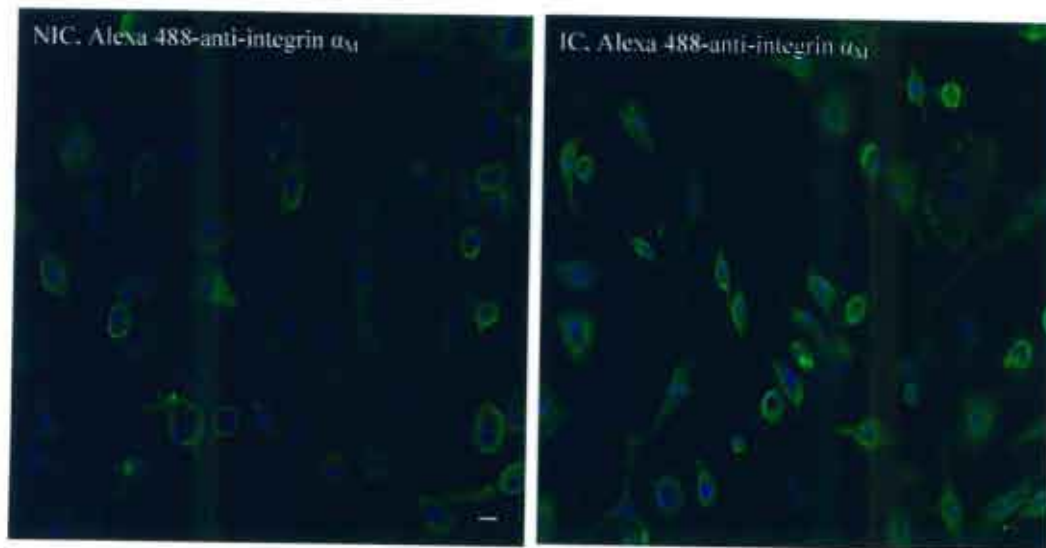


Figure 16. **Differential surface expression of integrin- α_M on macrophages in response to infection with *M. avium*.** At 7 days post-infection, non-infected cells (NIC) and *M. avium*-infected cells (IC) were stained with Alexa 488-conjugated anti-integrin- α_M antibody and then with DAPI as described in Materials and Methods. Blue indicates DAPI-stained nuclei. Green indicates staining by the Alexa 488-conjugated antibody. The scale bar represents 5 μm .

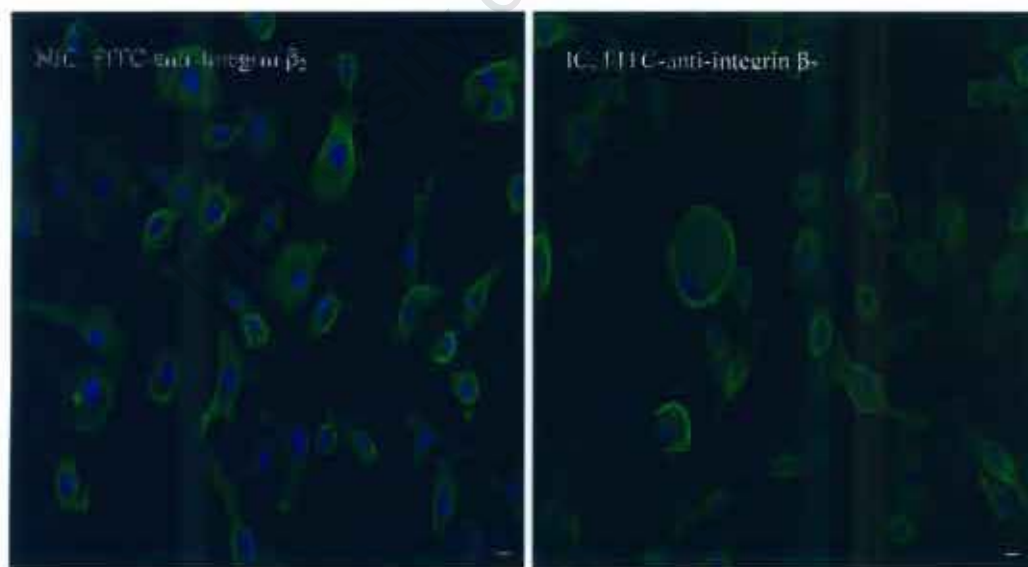


Figure 17. **Differential surface expression of integrin- β_2 on macrophages in response to infection with *M. avium*.** After 7 days of infection with or without *M. avium*, macrophages were stained with FITC-conjugated anti-integrin β_2 mAb followed by DAPI (blue stain) as described in Materials and Methods. Green indicates fluorescence from the FITC-conjugated antibody. Size bar represents 3 μm .

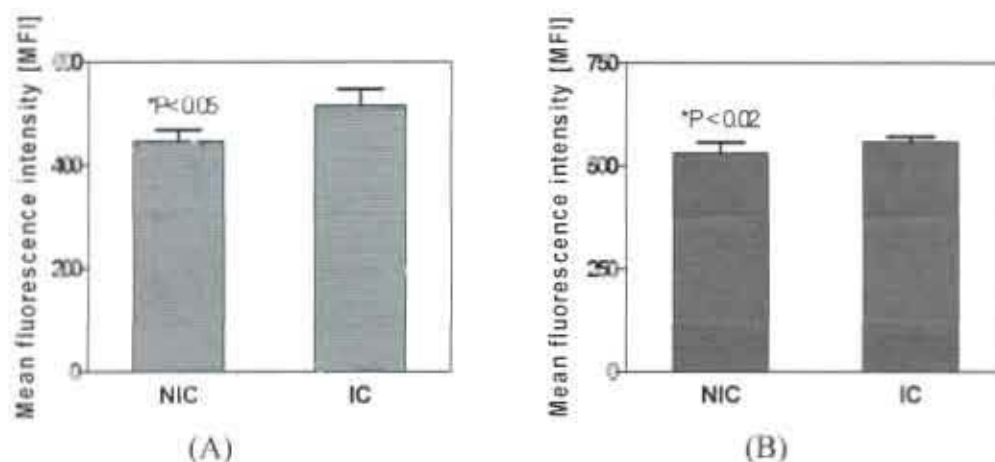


Figure 18. Cell-surface fluorescence intensity for integrin- α_M and integrin- β_2 in *M. avium*-infected and non-infected macrophages. At day 7 post-infection with or without *M. avium*, macrophages were stained for cell-surface expression of either integrin- α_M or integrin- β_2 as described in Materials and Methods. The mean fluorescence density was determined for triplicate slides per sample. $P < 0.05$ for integrin- α_M (A). $P < 0.02$ for integrin- β_2 (B).

2.2.7 Comparative whole cell staining for integrin- β_2 and - α_M in *M. avium*-infected and non-infected macrophages

Infection of mouse bone marrow-derived macrophages with *M. avium* caused an increased and a decreased surface expression of integrin- α_M and - β_2 respectively Fig 12. To determine if such observations denote an overall change in the total pool of either integrin- α_M or integrin- β_2 , *M. avium*-infected and non-infected macrophages at the same growth stage were first fixed and permeabilised with 0.5% Triton-X-100 as described in Materials and Methods. Both cell types were then stained with either FITC-conjugated anti-integrin- β_2 antibody or Alexa 488-conjugated anti-integrin- α_M antibody. The nuclei were stained with DAPI. Mean fluorescence intensity analysis for both staining (Fig. 19 and Fig. 20), revealed no significant difference for total protein pool of integrin- β_2 and

integrin- α_M between *M. avium*-infected and non-infected mouse bone marrow-derived macrophages (Fig. 21).

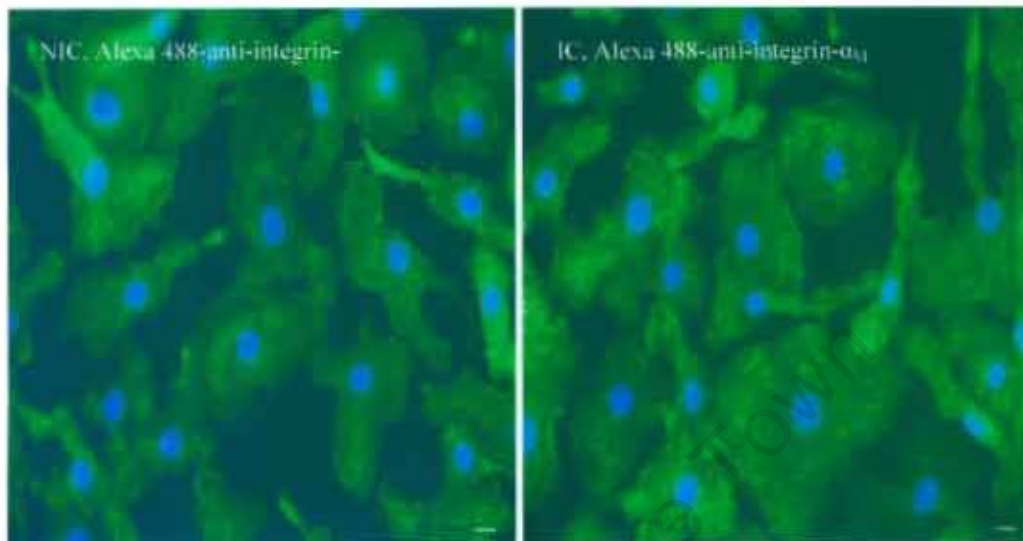


Figure 19. **Intracellular expression of integrin- α_M in macrophages in response to infection with *M. avium*.** After 7 days of infection with or without *M. avium*, macrophages were fixed, permeabilized, and stained with Alexa 488-conjugated anti-integrin- α_M monoclonal antibody as described in Materials and Methods. Blue indicates DAPI-stained nuclei. Green indicates fluorescence from the Alexa 488-conjugated antibody. The scale bar represents 1.5 μ m.

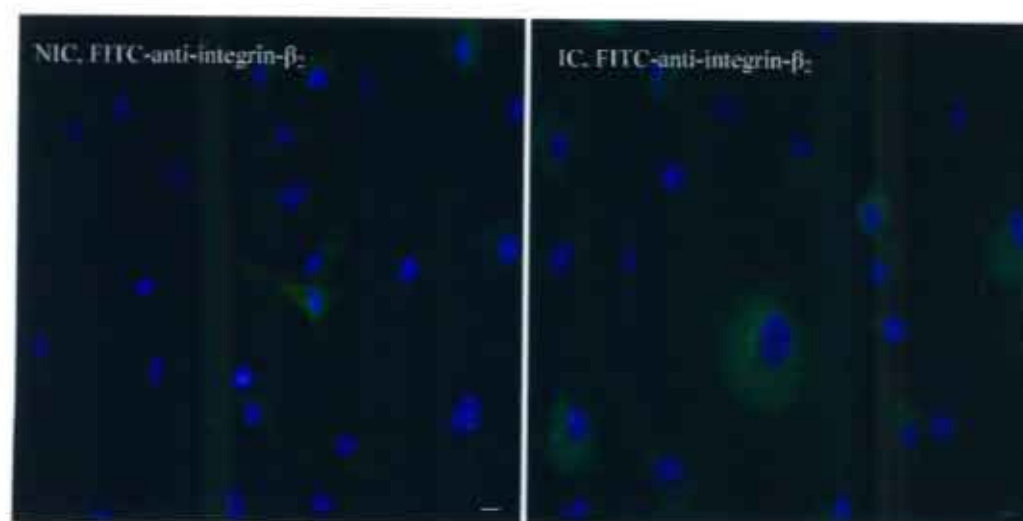


Figure 20. Intracellular expression of integrin- β_2 in macrophages in response to infection with *M. avium*. After 7 days of infection with or without *M. avium*, macrophages were fixed, permeabilized, and stained with Alexa 488-conjugated anti-integrin- β_2 monoclonal antibody as described in Materials and Methods. Blue indicates DAPI-stained nuclei. Green indicates fluorescence from the FITC-conjugated antibody. The scale bar represents 3 μ m.

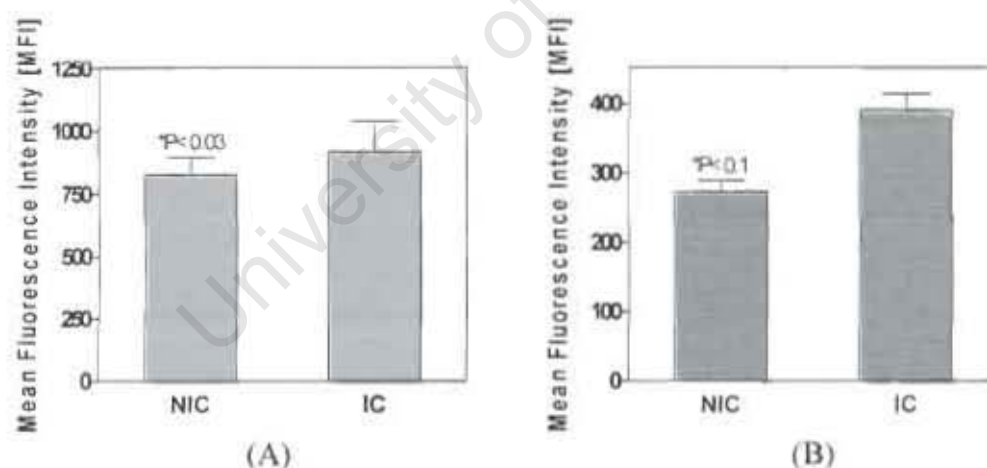


Figure 21. Intracellular fluorescence intensity for integrin- α_M and integrin- β_2 in *M. avium*-infected and non-infected macrophages. At day 7 post-infection with or without *M. avium*, macrophages were stained for intracellular levels of either integrin- α_M or integrin- β_2 as described in Materials and Methods. The mean fluorescence density was determined for triplicate slides per sample. $P < 0.03$ for integrin- α_M (A). $P < 0.1$ for integrin- β_2 (B).

2.2.8 Infection of macrophages with *M. avium* causes a redistribution of integrin- β_2 between the plasma membrane and intracellular membrane pools

Western blotting and RT-PCR analyses show that the effect of an altered surface expression of integrin- α_M and - β_2 on *M. avium*-infected macrophages is not at the protein synthesis or transcriptional level (Fig. 13 and Fig. 14). Subsequent immunofluorescence analysis for whole cell or cell-surface levels of either integrin- α_M or integrin- β_2 did not show a significant difference between *M. avium*-infected and non-infected cells. Because the immunostaining technique turned out to be insufficiently sensitive to detect a redistribution of integrin- β_2 away from the cell surface to intracellular membranes, we sought to compare infected and non-infected cells in terms of the intensity of surface-labelled integrin- β_2 to total integrin- β_2 as in Western blotting. ^{14}C -labelled membrane from *M. avium*-infected and non-infected cells were electrophoresed on SDS-PAGE and subjected to Western blotting analysis using anti-integrin- β_2 monoclonal antibody as described in Materials and Methods. Following exposure of the nitrocellulose membrane to X-ray film and autoradiography (Fig. 22), signal per amount of protein (slopes) of the integrin- β_2 band as from the X-ray film and autoradiography were determined for each sample (Fig. 23). The ratio of the slope from non-infected cells was about 2.3 fold more than that obtained from *M. avium*-infected macrophages (that is 450:200). This implies that in infected cells, of the total cellular amount of integrin- β_2 (as per Western blotting), less was on the cell surface to be labeled. No such analysis was done for integrin- α_M as no such commercially available antibodies obtained were suitable for Western blotting.

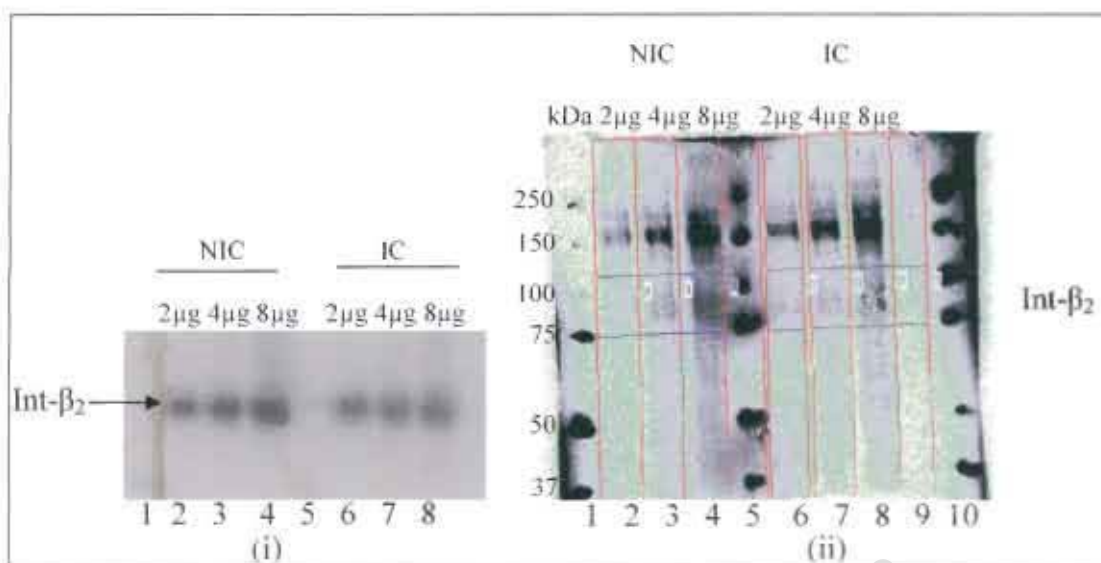


Figure 22. Western blotting followed by autoradiography of ^{14}C -labelled membrane glycoconjugates from *M. avium*-infected and non-infected cells. Two, four, and eight microgram of ^{14}C -labelled membrane proteins from *M. avium*-infected and non-infected cells were electrophoresed on SDS-PAGE and analysed by Western blotting for integrin- β_2 , (i). The nitrocellulose membrane was then subjected to autoradiography (ii). Lanes 2, 3, and 4 contained membrane proteins from non-infected cells (NIC). Lanes 6, 7, and 8 contained membrane proteins from *M. avium*-infected cells (IC). Lanes 1, 5, and 10 contained molecular weight-markers lined with ^{14}C -labelled pen.

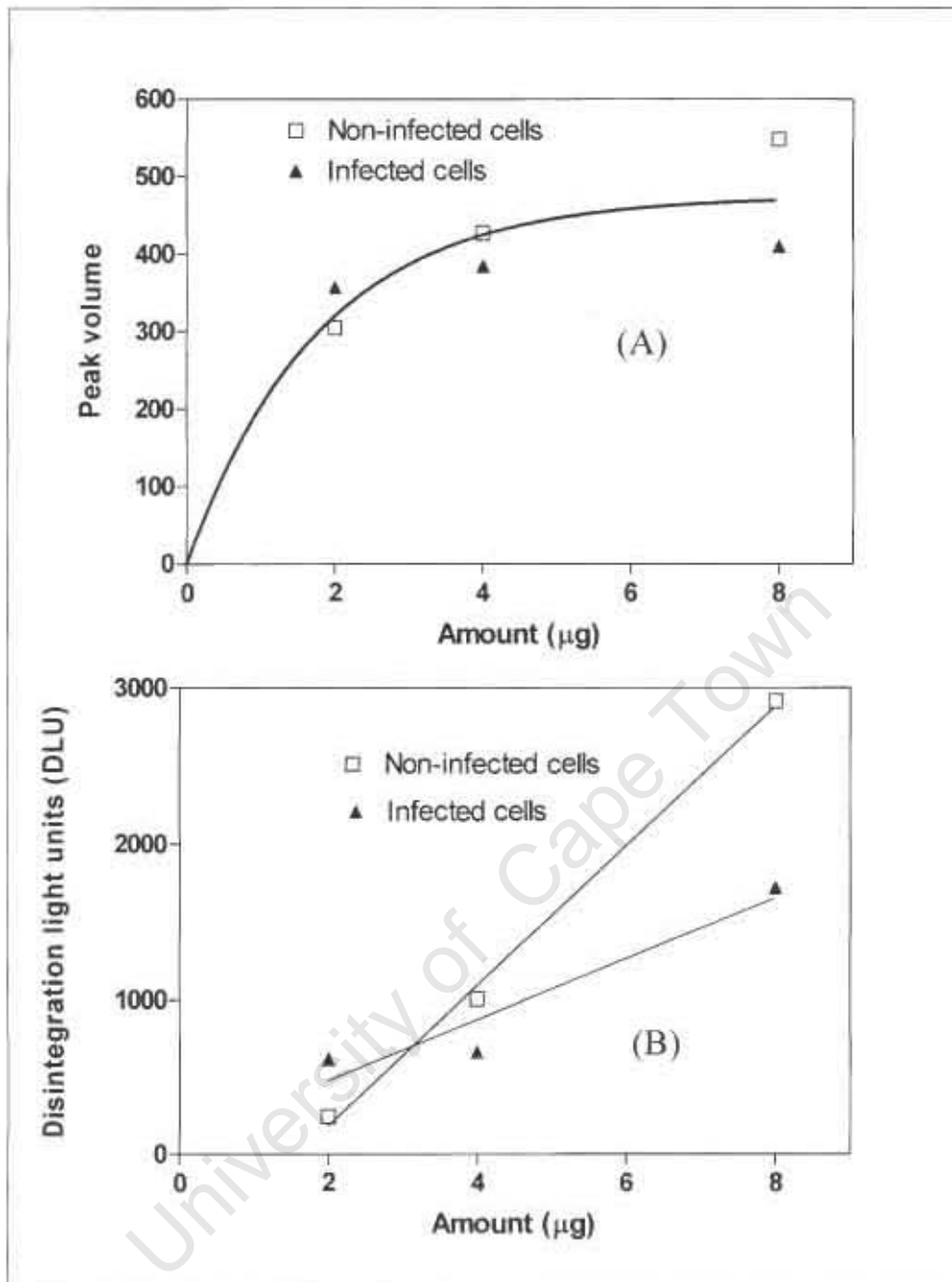


Figure 23. Intensities versus microgram plots of ^{14}C -labelled membrane proteins from *M. avium*-infected and non-infected cells. ^{14}C -labelled membrane from *M. avium*-infected and non-infected cells were subjected to Western blotting and autoradiography as shown in Fig. 26 The intensity of the integrin- β_2 band in each case was determined. These intensities were then plotted against amount of protein loaded in order to determine the intensity per microgram of protein. (A) Western blot densitometry plot. (B) Autoradiography intensity plot

2.2.9 Integrin- α_M co-immunoprecipitates with integrin- β_2 in *M. avium*-infected macrophages

Integrin- α_M and integrin- β_2 obligatorily occur as a heterodimer on the cell surface of macrophages, and as such represent the Mac-1 receptor. Infection of macrophages with *M. avium* caused a decreased and an increased surface expression of integrin- β_2 and integrin- α_M respectively (Fig. 12). Therefore, the question of an alternative possible dimerization partner for integrin- α_M in the context of reduced cell-surface expression of integrin- β_2 on *M. avium*-infected cells became obvious. In order to address this, *M. avium*-infected and uninfected macrophages were surface labelled with ^{14}C -

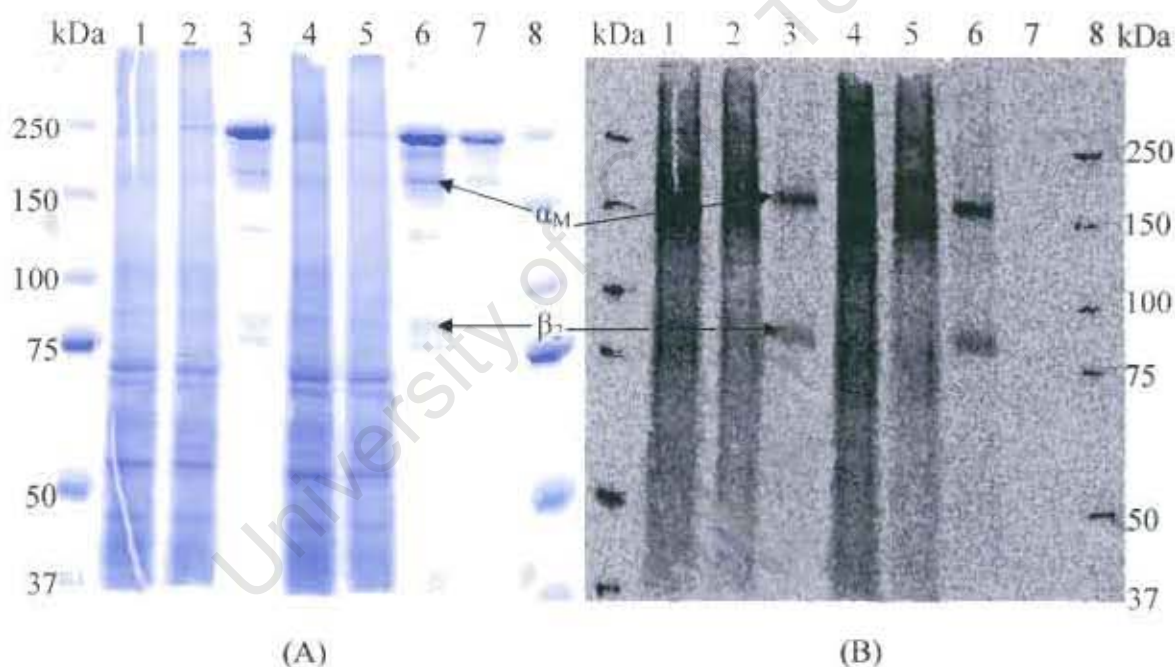


Figure 24. Co-immunoprecipitation of $\alpha_M\beta_2$ complex from *M. avium*-infected and non-infected macrophages with anti-integrin- α_M antibody. At 7days post-infection, *M. avium*-infected and non-infected cells were surface-labelled with ^{14}C -galactose, lysed, and $\alpha_M\beta_2$ complex was co-immunoprecipitated with anti-integrin α_M antibody. The immunoprecipitates were analysed on 7% SDS-PAGE under non-reducing conditions and exposed for autoradiography. (A) Coomassie-stained gel and (B) ^{14}C autoradiogram. Lanes 1, 2, and 3 are lysate, supernatant, and immunoprecipitate from non-infected cells. Lanes 4, 5, and 6 represent lysate, supernatant, and immunoprecipitate from *M. avium*-infected cells. Lanes 7 and 8 contained undenatured antibody and molecular-weight marker respectively.

galactose and separately subjected to co-immunoprecipitation using anti-integrin- α_M monoclonal antibody M1/70 as described in Materials and Methods. The immunoprecipitates and remaining supernatants from infected and uninfected cells were analyzed on 7% SDS-PAGE under non-denaturing conditions as in Fig. 24A. To specifically locate which bands on the immunoprecipitate from each cell type represent

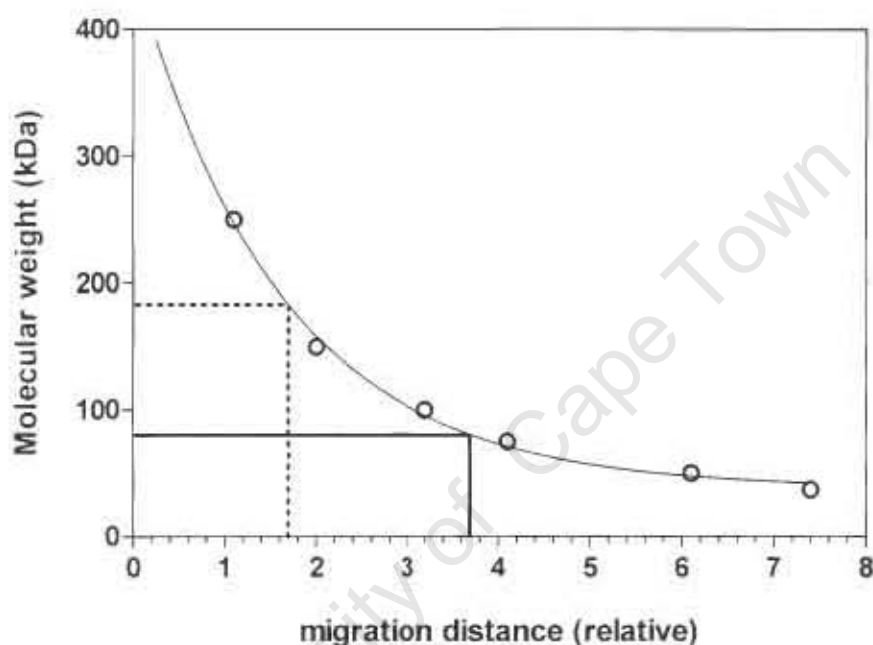


Figure 25. **Analysis of molecular weight of integrin- α_M and - β_2 chains on 7% SDS-PAGE after Co-immunoprecipitation.** After 7 days of infection of MBDM with (IC) or without (NIC) with *M. avium*, the cells were subjected to co-immunoprecipitation using anti-integrin- α_M monoclonal antibody M1/70. The immunoprecipitates from NIC and IC were analysed on 7% SDS-PAGE under non-denaturing conditions and Coomassie-stained. Molecular weights of integrin- α_M and - β_2 chains were determined by interpolating from a standard curve generated from known precision stain molecular-weight marker. Interpolated value for integrin- α_M band at ~182kDa; integrin- β_2 band at ~80kDa correspond to the molecular-weight of integrin- α_M and integrin- β_2 of 170kDa and 95kDa respectively.

those of either subunit as opposed to antibody bands, the Coomassie-stained gel (Fig. 24A) was exposed to cyclone phosphor imager as in Fig. 24B. By plotting a graph of

known molecular weights against migration distance of the molecular-weight markers (Fig. 25), the molecular weight of the unknown bands was obtained by interpolation. Bands appeared at the position expected for integrin- α_M and $-\beta_2$. No additional bands were observed for both cell types.

2.2.10 Culture medium from *M. avium*-infected macrophages causes an altered surface expression of integrin- α_M and $-\beta_2$ on non-infected macrophages

In order to determine if diffusible factors in the medium from infected macrophages could induce an increased and a decreased surface expression of integrin- α_M and integrin- β_2 , respectively, on non-infected macrophages, one-day-old medium from *M. avium*-infected macrophages was transferred onto non-infected macrophages on a daily basis over seven days. Plasma-membrane glycoproteins of both cell types were labelled with different isotopes and the membrane proteins were isolated as described in Materials and Methods. The samples were mixed and analyzed in the same lane on an SDS-PAGE. The lane was trypsinized and analyzed in a liquid-scintillation counter in order to obtain a radioactivity profile for both cell types. The profiles were normalized such that the same area was obtained under each curve. It was observed that the medium from *M. avium*-infected macrophages induced an increased and a decreased surface expression of integrin- α_M and $-\beta_2$ respectively, on non-infected macrophages (Fig. 26), as it was observed on *M. avium*-infected cells from the same experiment (Fig. 12).

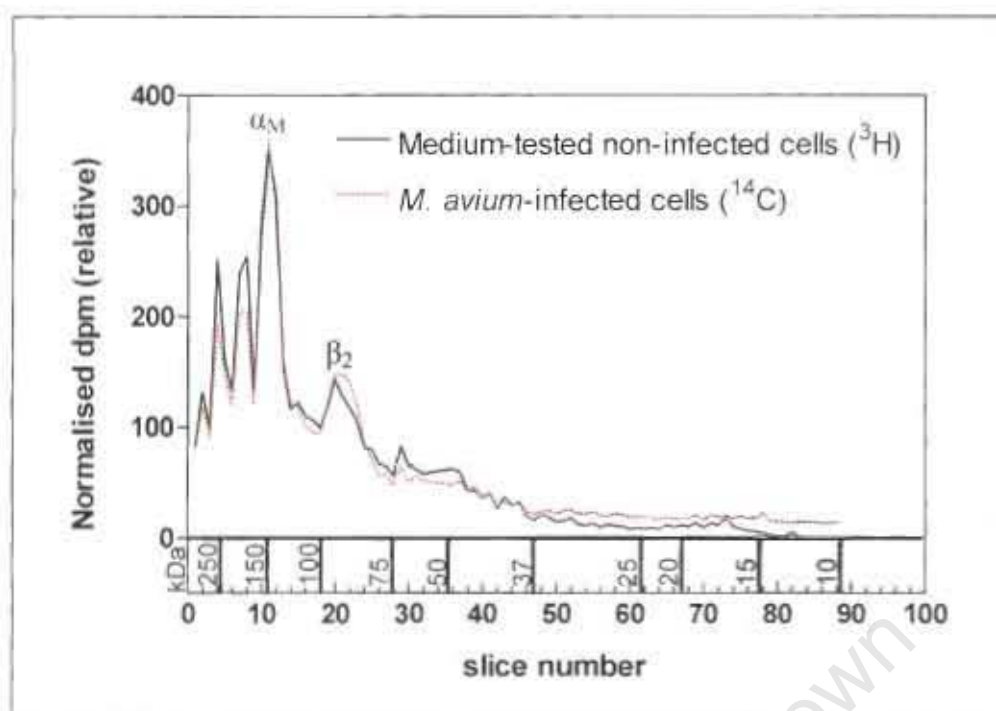


Figure 26: Effect of medium from *M. avium*-infected cells on the expression of integrin- β_2 and $-\alpha_M$ on non-infected cells. A mixture of ^{14}C - and ^3H -labelled plasma membrane proteins from *M. avium*-infected and medium-tested non-infected macrophages, respectively, was analyzed on an 8%-15% gradient SDS-PAGE. The lane was cut into 2.5mm wide slices that were then trypsinized as described in Material and Methods in order to release labelled protein fragments. The digestion from each slice was counted twice in a liquid-scintillation counter and an average taken. The amount of dpm from each slice was then plotted against slice number. Because the total counts for ^{14}C and ^3H were different, the profiles as shown were normalized such that the total areas under the curves were the same. The profile from medium-tested non-infected cells is identical to the one from *M. avium*-infected cells. This was obtained from the same experiment with that in Fig. 12

Chapter 3: DISCUSSION

In an *in vivo* mouse tuberculosis infection model and depending on the route of administration, it has been found that integrin- β_2 is down-regulated on macrophages (Bonato *et al.*, 2001) but up-regulated on T- and B- lymphocytes (Bonato *et al.*, 2002). Interestingly, we also observed in our *in vitro* study that infection of mouse bone marrow-derived macrophages with *M. avium* caused a differential expression of labelled cell-surface glycoproteins, particularly integrin- α_M being up-regulated close to about 40% and integrin- β_2 being down-regulated close to about 80% with a $T_{1/2} \approx 1.5$ days. By extrapolation, the change starts immediately after infection and becomes fully established after 7 days (Fig 1; Itoe, B.Sc(med)Honours thesis, 2004). The opposite trend for integrins- α_M and β_2 was unexpected, as integrins- α_M and β_2 exist as a heterodimer, known as Mac-1 or CR3. In the present study, we sought to determine the mechanism(s) for integrin- β_2 down-regulation and concurrent up-regulation of integrin- α_M on the surface of macrophages upon infection with pathogenic *M. avium*, and to delineate whether such changes as observed by Bonato *et al.* (2001) are restricted only to infected cells or could be transmitted to uninfected cells by factors secreted by infected cells. In addition, we also sought to identify any additional dimerization partner for integrin- α_M to compensate for the declining abundance of integrin- β_2 on the surface of infected cells.

Following optimization of techniques, it was important for us to confirm that macrophages were properly infected and that our previous finding for changes in surface expression of labelled glycoconjugates could be reproduced. Analysis of the distribution of both ^3H - and ^{14}C -labelled plasma-membrane proteins from non-infected and infected cells, respectively, across the gradient SDS-PAGE by trypsin ingel digestion followed by

liquid-scintillation counting (Fig. 12) revealed profiles that are in good agreement with our previous observation as in Fig. 1 (Itoe, B.Sc(med)Honours thesis, 2004), with integrin- α_M being up-regulated and integrin- β_2 being down-regulated. Electron-microscopy observation of *M. avium*-infected macrophages (Fig 9) matches with what has been previously reported by other authors for both *in vivo* and *in vitro* pathogenic *M. avium* infection models (Frehel *et al.*, 1986; de Chastellier *et al.*, 1995). The bacteria were intact (with a regular shape, an electron translucent membrane, and well organized cytoplasmic membrane), and actively replicated, there was an all-around close apposition of the phagosomal membrane to the bacterium cell wall (de Chastellier and Thilo, 1997; Pietersen *et al.*, 2004). No phagosome-lysosome fusion was observed.

To elucidate whether the changes observed in surface expression of both integrin- α_M and integrin- β_2 by the radiolabelling technique (Fig. 1) were as a result of a change in transcription or protein synthesis, RT-PCR and Western-blot experiments were carried out. For PCR, primers specific to integrin- β_2 and - α_M genes were designed for exon 5 and 29 respectively to overlap the intron-exon boundaries of the preceding and proceeding exon. No difference was observed for integrin- β_2 gene expression between infected and non-infected cells ($P < 0.04$; Fig. 14). The PCR results for integrin- β_2 corroborated our Western blotting results where no significant difference was observed for integrin- β_2 expression in infected and non-infected cells (Fig. 13). No Western blotting analysis was performed for integrin- α_M expression because the antibodies that were commercially available were not suitable for this purpose.

Alexa 488-conjugated anti-integrin- α_M or FITC-conjugated anti-integrin- β_2 antibodies were used in immunostaining assays to determine cell-surface and intracellular levels of either integrin- α_M or integrin- β_2 in infected and non-infected cells. Integrin- α_M and integrin- β_2 form a heterodimer and are usually expressed on more mature cells of murine hematopoietic stem cells (Miller *et al.*, 1985, 1986). In addition to exo-galactosylation, results for immunostaining for cell-surface expression of integrin- α_M and integrin- β_2 on infected and non-infected macrophages were shown in Fig 16 and 17. Though visually different, mean fluorescence intensity analysis did not show any significant difference between infected and non-infected cells, with a $P < 0.05$ for integrin- α_M and a $P < 0.02$ for integrin- β_2 (Fig. 18). The immunofluorescence staining appeared to be less sensitive to detect differential changes in surface expression of either antigen, because the results did not correlate with those obtained by exo-galactosylation. Our attempts to trypsinize the macrophages and subject them to FACS analysis were unsuccessful. The macrophages were too resistant to the action of trypsin and we also feared that trypsin might cleave off our proteins of interest before the staining protocol. Because the staining observed in Fig. 16 and Fig. 17 are not homogenous, we proposed to first stain for intracellular *M. avium* on infected cells with an anti-*M. avium*, conjugated to a different fluorochrome other than Alexa 488 and FITC, before staining for cell-surface expression of either integrin antigens. This could not be performed because no antibody was available. Alternatively, mycobacteria could have been stained with PKH26 red before infection of macrophages. .

For us to be able to match our observations for surface-labelled glycoconjugates to that of the intracellular levels of either antigen in the context of a redistribution of either

antigen between plasma membrane and intracellular pools, infected and non-infected cells were fixed with 4% paraformaldehyde, permeabilised with 0.5% Triton-X-100 for 5 minutes, and then stained with either antibody (Fig. 17 and Fig. 18). Mean fluorescence intensity analysis did not show any significant difference in intracellular levels of integrin- α_M and integrin- β_2 antigens ($P < 0.03$ and $P < 0.1$ respectively; Fig. 19) between *M. avium*-infected and non-infected cells. However, for integrin- α_M , the proteins appeared to be more concentrated on the cytoplasmic side of the plasma membrane as opposed to being in other cell organelles.

The insensitivity of the fluorescence technique in detecting differential surface or whole cell expression of either antigen could reflect a possible effect of fixation and permeabilization on the conformation of CR3 protein. This could have been checked by either doing fixation or permeabilization for a shorter time than we have used.

Mycobacterial lipopolysaccharides (LPS) have been shown to interact with specific moieties on the CR3 receptor (Cywes *et al.*, 1997). This interaction triggers several intracellular signalling cascades that can result in changes in transcription. Our semi-quantitative RT-PCR results (Fig. 14) compliments the result obtained from the Western blot experiment for integrin- β_2 (Fig. 13). This implies that our observations of an increased and a decreased surface expression of integrin- α_M and integrin- β_2 (Fig. 12) respectively, could only be as a result of translocation of pre-existing pool from one cellular compartment to another. Interestingly, Todd *et al.*, 1984 and Bainton *et al.*, 1987 have shown that in addition to being present on the plasma membrane, Mac-1, is also stored in a latent intracellular pool, peroxidase-negative granules. Studies by Miller *et al.*, 1987, also showed that stimulation of monocytes with *formyl*-methionyl-leuccyl-

phenylalanine (fMLP), tumour necrosis factor (TNF), and platelet-derived growth factor (PDGF) caused mobilization of Mac-1 from the intracellular pool to the plasma membrane. Together with these studies, our findings suggest that infection of macrophages with *M. avium* caused a redistribution of integrin- α_M and integrin- β_2 proteins between the plasma membrane and the intracellular pools.

To obtain a more sensitive method to determine redistribution of integrin- β_2 away from the cell surface, we designed experiments where we could observe a decrease in the ratio of the intensities of surface-labelled integrin- β_2 band to the signal from Western blot analysis. Our analysis shows a 2.3-fold (450:200) difference in this ratio when comparing non-infected cells to infected cells. Though these might reflect the redistribution effect, there is significant error associated with each of the values. Nonetheless, this result implies that despite of no overall change in protein synthesis or transcription (Fig. 13 and Fig. 14), synthesized integrin- β_2 was not being translocated to the plasma membrane. No such analysis was done for integrin- α_M because there was no antibody available for Western blot analysis of integrin- α_M on membrane proteins from non-infected and infected cells. Alternatively, the redistribution effect could be demonstrated by overexpressing different fluorescently tagged proteins in a macrophage cell lineage, subjecting the cells to infection, and then monitoring the distribution of the proteins under live imaging. Non-infected cells in the vicinity should serve as a control.

In an *in vivo* mouse infection model, Bonato *et al.*, 2001, reported that integrin- β_2 is down-regulated on macrophages following intra-peritoneal infection with *M. tuberculosis*. However, these authors did not delineate whether such effects are unique only to infected macrophages or both infected and non-infected macrophages. To clear

this doubt, we tested if the changes observed in Fig. 12 could occur on non-infected cells as a result of factors being secreted by infected cells. We obtained a similar profile as it is for infected cells, with integrin- α_M being up-regulated and integrin- β_2 being down-regulated. This raises the question of what could be the identity of such factor(s). Among many of the cytokines that are released upon activation of macrophages and are said to have an effect on surface expression of integrin is tumor necrosis factor (TNF) (Bainton *et al.*, 1987). However, TNF is released from *M. avium*-infected cells robustly and its production levels off just after 2 days of infection. Therefore, the production of the factor responsible for this change needs to be continuous in order to sustain the effect until day 7 or 8 post-infection; as such changes have been determined in our previous study (Itoe, B.Sc(med)Honours thesis, 2004). For identification of the secreted factor, culture medium from infected cells needs to be fractionated according to different molecular sizes and tested for their effect on non-infected cells as in Fig 12 and 26.

In addition to the β_2 integrin family, other β integrin families, β_1 , β_3 , β_4 , β_5 , β_6 , β_7 , and β_8 exist on different cell types with β_2 and β_7 mostly restricted to white blood cells (review by Hynes, 2002). Our co-immunoprecipitation analysis showed that integrin- β_2 remained associated to integrin- α_M (Fig. 21 and Fig. 22). No substitute for reduced integrin- β_2 on infected macrophages was observed.

4.2 Implication of results

Overall, what could be the significance of altered surface expression of integrin- α_M and integrin- β_2 on infected macrophages? In our view, this would mean a decreased intercellular contact between CR3 on infected macrophages and ICAM-1 and ICAM-2 on

T-lymphocytes. Such interactions are important in driving cytolytic T-lymphocytes response and cytokine production, both of which are very central in eliminating invading pathogens. Activation of CR3 triggers intracellular signaling events that lead to changes in gene expression, particularly the production of cytokines. As it has been reviewed, the cytokines play a very central role in the development of granulomatous lesion at the site of infection. A decrease or an altered surface expression of CR3 could adversely affect production of cytokines and would favorably support the intracellular survival of pathogenic mycobacteria. A decrease in cytokine production could have an effect on the time course and morphology granuloma formation.

4.1 Conclusion and future perspectives

We have demonstrated in our *in vitro* model that infection of macrophages with *M. avium* caused an altered surface expression of integrin- α_M (up-regulated) and integrin- β_2 (down-regulated) as a result of a redistribution of integrin- α_M and integrin- β_2 between plasma membrane and intracellular pools. Such changes can also be brought about on non-infected cells by factors secreted into the medium from infected cells. Despite the declining abundance of integrin- β_2 on the cell surface of infected cells, no other dimerization partner for integrin- α_M was observed.

Future work should focus on identifying the factors responsible for these changes on infected cells. Factors such as the state of the bacteria (virulent or avirulent, and death or live bacteria), bacterial lipopolysaccharides should be tested for their possible effect on non-infected cells. The identity of the secreted factors from infected cells that caused the change on non-infected cells should also be investigated by fractionating the medium

from infected cells according to molecular sizes and testing their effect on non-infected cells as in Fig. 12 and Fig. 13. The macrophages should also be stimulated with known factors such as *formyl*-methionyl-leucyl-phenylalanine (fMLP), tumor necrosis factor (TNF), and platelet-derived growth factors (PDGF) and their effects determined by exogalactosylation and immunofluorescence. Also, it could be necessary to determine changes in glycosylation pattern of integrin- α_M and integrin- β_2 that might have occurred as a result of infection. This could help to explain the difference obtained from radioactivity profile of membrane proteins from infected cells.

The CR3 receptor is the main receptor for the uptake of pathogenic mycobacteria. An altered surface expression of CR3 should protect the host cells against secondary infection. This could be investigated by infecting already infected cells with complement opsonised or non-opsonised zymosan and GFP-tagged mycobacteria and then monitor the uptake of the particle. Also, secretion of cytokines by cells treated with medium from infected cells could be investigated. The role of CR3 for subsequent survival of mycobacteria could also be determined by infecting CHO cells expressing Mac-1 and macrophages from CR3 knock-out mice..

References

1. Altieri, D.C., Bader, R., Mannucci, P.M., and Edgington, T.S. (1988). Oligospecificity of the Cellular Adhesion Receptor MAC-1 Encompasses an Inducible Recognition Specificity for Fibrinogen. *J. Cell Biol.* **107**, 1893-1900
2. Allen, L.A.H., and Aderem, A. (1996) Mechanisms of phagocytosis. *Curr. Opin. Immunol.* **8**, 36
3. Armstrong, J.A. and D'Arcy Hart, P. (1971). Response of cultured macrophages to *Mycobacterium tuberculosis*, with observations on fusion of lysosomes with phagosomes. *J. Exp. Med.* **134**, 713-740
4. Bainton, D.F., Miller, L.J., Kishimoto, T.K., and Springer, T.A. (1987). Leukocyte adhesion receptors are stored in peroxidase-negative granules of human neutrophils. *J. Exp. Med.* **166**, 1641-1653
5. Beller, D.I., Springer, T.A., and Schreiber, R.D. (1982). Anti-Mac-1 Selectively Inhibits the Mouse and Human Type Three Complement Receptor. *J. Exp. Med.* **156**, 1000-1009
6. Bermudez, L.E., Goodman, J., and Petrofsky, M. (1999). Role of Complement Receptors in Uptake of *Mycobacterium avium* by Macrophages In Vivo: Evidence from Studies Using CD18-Deficient Mice. *Infection and Immunity.* **67**, 4912-4916
7. Bohnsack, J.F., and Zhou, X.N. (1992). Divalent cation substitution reveals CD18- and very late antigen- dependent pathways that mediate human neutrophil adherence to fibronectin. *J. Immunol.* **149**, 1340-1347

8. Bonato, V.L.D., Medeiros, A.I., Lima, M.F., Dias, A.R., Faccioli, L.H. and Silva, C.L. (2001). Downmodulation of CD18 and CD86 on Macrophages and VLA-4 on Lymphocytes in Experimental Tuberculosis. *Scand. J. Immunol.* **54**, 564-573
9. Bonato, V.L., Goncalves, E.D., Santos, R.R. and Silva, C.L. (2002). Genetic aspects and microenvironment affect expression of CD18 and VLA-4 in experimental tuberculosis. *Scand. J. Immunol.* **56**, 185-194
10. Bourne, H.R., Sanders, D.A., and McCormick, F. (1991). The GTPase superfamily: conserved structure and molecular mechanism. *Nature* **349**, 117-127
11. Bradford, M.M. (1976). A rapid and sensitive method for the quantitation of microgram quantities of protein utilizing the principle of protein-dye binding. *Anal Biochem.* **72**, 248-254
12. Bucci, C., Parton, R.G., Mather, I.H., Stunnenberg, H., Simons, K., Hoflack, B. and Zerial, M. (1992). The small GTPase rab5 functions as a regulatory factor in the early endocytic pathway. *Cell* **70**, 715-728
13. Bucci, C., Thomsen, P., Nicoziani, P., McCarthy, J., and van Deurs, B. (2000). Rab7, a key to lysosome biogenesis. *Mol. Biol. Cell* **11**, 467-480
14. Chavrier, P., Parton, R.G., Hauri, H.P., Simons, K., and Zerial, M. (1990). Localization of low molecular weight GTP binding proteins to exocytic and endocytic compartments. *Cell* **62**, 317-329
15. Clemens, D.L. and Horwitz, M.A. (1995). Characterization of the *Mycobacterium tuberculosis* phagosome and evidence that phagosomal maturation is inhibited. *J. Exp. Med.* **181**, 257-270

16. Clemens, D.L. and Horwitz, M.A. (1996). The *Mycobacterium tuberculosis* phagosome interacts with early endosomes and is accessible to endogenously administered transferrin. *J. Exp. Med.* **184**, 1349-1355
17. Cywes, C., Godenir, N.L., Hoppe, H.C., Scholle, R.R., Steyn, L.M., Kirsch, R.E., and Ehlers, M.R.W. (1996) Nonopsonic Binding of *Mycobacterium tuberculosis* to Human Complement Receptor Type 3 Expressed in Chinese Hamster Ovary Cells. *Infect. Immunity.* **64**, 5373-5383
18. Cywes, C., Hoppe, H.C., Daffé, M., and Ehlers, M.R.W (1997). Nonopsonic Binding of *Mycobacterium tuberculosis* to Complement Receptor Type 3 Is Mediated by Capsular Polysaccharides and Is Strain Dependent. *Infect. Immunity.* **65**, 4258-5383
19. de Chastellier, C., Lang, T. and Thilo, L. (1995). Phagocytic processing of the macrophage endoparasite, *Mycobacterium avium*, in comparison to phagosomes which contain *Bacillus subtilis* or latex beads. *Eur. J. Cell Biol.* **68**, 167-182
20. de Chastellier, C. and Thilo, L. (1997). Phagosome maturation and fusion with lysosomes in relation to surface property and size of the phagocytic particle. *Eur. J. Cell Biol.* **74**, 49-62
21. de Chastellier and Thilo, L. (2002). Pathogenic *Mycobacterium avium* remodels the phagosome membrane in macrophages within days after infection. *Eur. J. Cell Biol.* **81**, 17-25
22. Defacque, H., Egeberg, M., Habermann, A., Diakonova, M., Roy, C., Mangeat, P., Voeller, W., Marriot, G., Plannstiel, J., Faulstich, H., and Griffiths, G. (2000). Involvement of ezrin/moesin in de novo actin assembly on phagosomal membranes. *EMBO J.* **19**, 199-212

23. Desjardins, M., Huber, L.A., Parton, R.G. and Griffiths, G. (1994). Biogenesis of Phagolysosomes Proceeds through a Sequential Series of Interactions with the Endocytic Apparatus. *J. Cell Biol.* **124**, 677-688
24. Diamond, M.S., Staunton, D.E., de Fougères, A.R., Stacker, S.A., Garcia-Aguilar, J., Hibbs, M.L., and Springer, T.A. (1990). ICAM-1 (CD54): A Counter-Receptor for Mac-1 (CD11b/CD18). *J. Cell Bio.* **111**, 3129-3139
25. Dye, C., Scheele, S., and Dolin, P. (1999). Global burden of tuberculosis: estimated incidence, prevalence, and mortality by country. *JAMA* **282**, 677-686
26. Feng, Y., Press, B. and Wandinger-Ness, A. (1995). Rab7: an important regulator of late endocytic membrane traffic. *J. Cell Biol.* **131**, 1435-1452
27. Ferrari, G., Langen, H., Naito, M. and Pieters, J. (1999). A Coat Protein on Phagosomes Involved in the Intracellular Survival of Mycobacteria. *Cell* **97**, 435-447
28. Flaherty, S.F., Golenbock, D.T., Milham, F.H., Ingalls, R.R. (1997). CD11/CD18 Leukocyte Integrins: New Signaling Receptors for Bacterial Endotoxin. *J. Surgical Research.* **73**, 85-89
29. Flynn, J. and Chan, J. (2005). What's good for the host is good for the bug. *Trends Microbiol.* **13**, 98-102
30. Fratti, R.A., Backer, J.M., Gruenberg, J., Corvera, S., and Deretic, V. (2001). Role of phosphatidylinositol-3-kinase and rab5 effectors in phagosomal biogenesis and mycobacterial phagosome maturation arrest. *J. Cell Biol.* **154**, 631-644
31. Fratti, R.A., Chua, J. and Deretic, V. (2002). Cellubrevin Alterations and *Mycobacterium tuberculosis* Phagosome Maturation Arrest. *J. Biol. Chem.* **277**, 17320-17326

32. Frehel, C., de Chastellier, C., Lang, T. and Rastogi, N. (1986). Evidence for inhibition of fusion of lysosomal and prelysosomal compartments with phagosomes in macrophages infected with pathogenic *Mycobacterium avium*. *Infect. Immun.* **52**, 252-262.
33. Frehel, C., de Chastellier, C., Offredo, C., and Berche, P. (1991). Intramacrophage Growth of *Mycobacterium avium* during Infection of Mice. *Infect. Immun.* **59**, 2207-2214
34. Frehel, C., Offredo, C., and de Chastellier, C. (1997). The Phagosomal Environment Protects Virulent *Mycobacterium avium* from Killing and Destruction by Clarithromycin. *Infect. Immunity* **65**, 2792-2802
35. Frehel, C., Cannone-Hergaux, F., Gros, P. and de Chastellier, C. (2002). Effect of *Nramp1* on the bacterial replication and on maturation of *Mycobacterium avium*-containing phagosomes in bone marrow-derived mouse macrophages. *Cellular Microbiology* **4**, 541-556
36. Galli, T., Chilcote, T., Mundigl, O., Binz, T., Niemann, H. and de Camilli, P. (1994). Tetanus toxin-mediated cleavage of cellubrevin impairs exocytosis of transferrin receptor-containing vesicles in CHO cells. *J. Cell Biol.* **125**, 1015-1024
37. Gaullier, J.M., Simonsen, A., D'Arrigo, A., Bremnes, B., Stenmark, H. and Aasland, R. (1998). FYVE fingers bind PtdIns(3)P. *Nature* **394**, 432-433
38. Goodman, T.G. and Bajt, M.L. (1996). Identifying the Putative Metal Ion-dependent Adhesion Site in the β_2 (CD18) Subunit Required for $\alpha_L\beta_2$ and $\alpha_M\beta_2$ Ligand Interactions. *J. Biol. Chem.* **271**, 23729-23736

39. Gorvel, J.P., Chavrier, P., Zerial, M., and Gruenberg, J. (1991). Rab5 controls early endosome fusion in vitro. *Cell* **64**, 915-925
40. Grabbe, S., Varga, G., Beissert, S., Steinert, M., Pendl, G., Seeliger, S., Bloch, W., Peters, T., Schwarz, T., Sunderkötter, C., and Scharffetter-Kochanek, K. (2002). β_2 integrins are required for skin homing of primed T cells but not for priming naïve T cells. *J. Clin. Invest.* **109**, 183-192
41. Guérin, I. and de Chastellier, C. (2000). Pathogenic Mycobacteria Disrupt the Macrophage Actin Filament Network. *Infect. Immun.* **68**, 2655-2662
42. Guérin, I. and de Chastellier, C. (2000). Disruption of the actin filament network affects delivery of endocytic contents marker to phagosomes with early endosome characteristics: The case of phagosomes with pathogenic mycobacteria. *Eur. J. Cell Biol.* **79**, 735-749
43. Harris, E.S., McIntyre, T.M., Prescott, S.M., and Zimmerman, G.A. (2000). The Leukocyte Integrins. *J. Biol. Chem.* **275**, 23409-23412
44. Hu, C., Mayadas-Norton, T., Tanaka, K., Chan, J., and Salgame, P. (2000). *Mycobacterium tuberculosis* Infection in Complement Receptor 3-Deficient Mice. *J. Immunol.* **165**, 2596-2602
45. Hu, C., Ahmed, M., Melia, T.J., Söllner, T.H., Mayer, T., and Rothman, J.E. (2003). Fusion of cells by flipped SNAREs. *Science*. **300**, 1745-1749
46. Hughes, P.E., Diaz-Gonzalez, F., Leong, L., Wu, C., McDonald, J.A., Shattil, S.J., and Ginsberg, M.H. (1996). Breaking the Integrin Hinge. *J. Biol. Chem.* **271**, 6571-6574

47. Hynes, R.O. (2002). Integrins: Bidirectional, Allosteric Signaling Machines. *Cell* **110**, 673-687
48. Ingalls, R.R., and Golenbock, D.T. (1995). CD11c/CD18, A Transmembrane Signaling Receptor for Lipopolysaccharide. *J. Exp. Med.* **181**, 1473-1479
49. Kaplan, G. (1977). Differences in the mode of phagocytosis with Fc and C3 receptors in macrophages. *Scand. J. Immunol.* **6**, 797
50. Kaufman, S.H.E. (2002). Protection against tuberculosis: cytokines, T cells, and macrophages. *Ann Rheum Dis.* **61**, 54-58
51. Kelley, V.A. and Schorey, J. (2003). *Mycobacterium's* Arrest of Phagosome Maturation in Macrophages Requires Rab5 Activity and Accessibility to Iron. *Mol. Biol. Cell* **14**, 3366-3377
52. Kürzinger, K., and Springer, T.A. (1982). Purification and Structural Characterization of LFA-1, a lymphocyte Function-associated Antigen, Mac-1, a Related Macrophage Differentiation Antigen Associated with the Type Three Complement Receptor. *J. Biol. Chem.* **257**, 12412-12418
53. Law, S.K., Fearon, D.T., and Levine, R.P. (1977). Action of the C3b-Inactivator on Cell-Bound C3b. *J. Immunol.* **122**, 759-765
54. Lawe, D.C., Patki, V., Heller-Harrison, R., Lambright, D. and Corvera, S. (2000). The FYVE Domain of Early Endosome Antigen 1 Is Required for Both Phosphatidylinositol-3-Phosphate and Rab5 Binding. *J. Biol. Chem.* **275**, 3699-3705
55. Le Cabec, V., Carréno, S., Moisand, A., Bordier, C., and Maridonneau-Parini, I. (2002). Complement Receptor 3 (CD11b/CD18) Mediates Type I and Type II

- Phagocytosis During Nonopsonic and Opsonic Phagocytosis, Respectively. *J. Immunol.* **169**, 2003-2009
56. Livak, K.J. and Schmittgen, T.D. (2001). Analysis of Relative Gene Expression Data Using Real-Time Quantitative PCR and the $2^{-\Delta\Delta C_T}$ Method. *Methods.* **25**, 402-408
57. Marlin, S.D., Morton, C.C., Anderson, D.C., and Springer, T.A. (1986). LFA-1 immunodeficiency disease: Definition of the genetic defect and chromosomal mapping of α and β subunits of the lymphocyte function-associated antigen (LFA-1) by complementation in hybrid cells. *J. Exp. Med.* **164**, 855-867
58. Mayorga, L.S., Bertini, F., Stahl, P.D. (1991). Fusion of Newly Formed Phagosomes with Endosomes in Intact Cells and in a Cell-free System. *J. Biol. Chem.* **266**, 6511-6517
59. Maske, C.P., Hollinshead, M.S., Higbee, N.C., Bergo, M.O., Young, S.G., and Vaux, D.J. (2003). A carboxyl-terminal interaction of lamin B1 is dependent on the CAX endoprotease Rce1 and carboxymethylation. *J. Cell Biol.* **162**, 1223-1232
60. Merion, M. and W.S. Sly (1983). The role of intermediate vesicles in the adsorptive endocytosis and transport of ligand to lysosomes by human fibroblasts. *J. Cell. Biol.* **96**, 644-650
61. Miller, L.J., Schwarting, R., and Springer, T.A. (1986). Regulated expression of the Mac-1, LFA, p150,95 glycoprotein family during leukocyte differentiation. *J. Immunol.* **137**, 2891-2900
62. Miller, L.J., Bainton, D.F., Borregaard, N., and Springer, T.A. (1987). Stimulated Mobilisation of Monocyte Mac-1 and p150,95 Adhesion Proteins from an Intracellular Vesicular Compartment to the Cell Surface. *J. Clin. Invest.* **80**, 535-544

63. Mobberley-Schuman, P.S. and Weiss, A.A. (2005). Influence of CR3 (CD11b/CD18) Expression on Phagocytosis of *Bordetella pertussis* by Human Neutrophils. *Infection and Immunity*. **73**, 7317-7323
64. Möller, W., Nemoto, I., Matsuzaki, T., Hofer, T. and Heyder, J. (2000). Magnetic Phagosome Motion in J774A.1 Macrophages: Influence of Cyhtoskeletal Drugs. *Biophys. J.* **79**, 720-730
65. Mu, F.T., Callaghan, J.M., Steele-Mortimer, O., Stenmark, H., Parton, R.G., Camphell, P.L., McCluskey, J., Yeo, J.P, Tock, E.P. and Toh, B.H. (1995). EEA1, an Early Endosome-Associated Protein. EEA1 is a conserved α -helical peripheral membrane protein flanked by cystein 'fingers' and contains a calmodulin-binding IQ motif. *J. Biol. Chem.* **270**, 13503-13511
66. Nielsen, E., Severin, F., Backer, J.M., Hyman, A.A. and Zerial, M. (1999). Rab5 regulates motility of early endosomes on microtubules. *Nat Cell Biol.* **1**, 376-382
67. Oh, Y., and Swanson, J.A. (1996). Different Fates of Phagocytosed Particles after Delivery into Macrophage Lysosomes. *J. Cell Biol.* **132**, 585-593
68. Patki, V., Virbasius, J., Lane, W.S., Toh, B.H., Shpetner, H.S. and Corvera, S. (1997). Identification of an early endosomal protein regulated by phosphatidylinositol-3-kinase. *Proc. Natl. Acad. Sci. USA* **94**, 7326-7330
69. Peyron, P., Bordier, C., N'Diaye, E.N., and Maridonneau-Parini, I. (2000). Nonopsonic Phagocytosis of *Mycobacterium kansasii* by Human Neutrophils Depends on Cholesterol and Is Mediated by CR3 Associated with Glycosylphosphatidylinositol-Anchored Proteins. *J. Immunol.* **165**, 5186-5191

70. Pietersen, R., Thilo, L. and de Chastellier, C. (2004). *Mycobacterium tuberculosis* and *Mycobacterium avium* modify the composition of the phagosomal membrane in infected macrophages by selective depletion of cell surface-derived macrophages. *Eur. J. Cell Biol.* **83**, 153-158
71. Pitt, A., Mayorga, L.S., Stahl, P.D., and Schwartz, A.L. (1992). Alterations in the Protein Composition of Maturing Phagosomes. *J. Clin. Invest.* **90**, 1978-1983
72. Pitt, A., Mayorga, L.S., Schwartz, A.L., and Stahl, P.D. (1992). Transport of Phagosomal Components to an Endosomal Compartment. *J. Biol. Chem.* **267**, 126-132
73. Reyes-Reyes, M., Mora, N., Gonzalez, G., and Rosales, C. (2002). β_1 and β_2 integrins activate different signaling pathways in monocytes. *Biochem. J.* **363**, 273-280
74. Rieder, H.L., Cauthen, G.M., Kelly, G.D., Bloch, A.B., and Snider, D.E. (1989). Tuberculosis in the United States. *JAMA.* **263**, 385-389
75. Rooyackers, A.W.J., Stokes, R.W. (2005). Absence of complement receptor 3 results in reduced binding and ingestion of *Mycobacterium tuberculosis* but has no significant effect on the induction of reactive oxygen intermediates or on the survival of the bacteria in resident and interferon-gamma activated macrophages. *Microbial Pathogenesis* **39**, 57-67
76. Russell, D.G. (2007). Who puts the tubercle in tuberculosis? *Nat. Rev. Microbiol.* **5**, 39-46
77. Sanchez-Madrid, F., Nagy, J., Robbins, E., Simon, P., and Springer, T.A. (1983). A human leukocyte differentiation antigen family with distinct alpha subunits and a common beta subunit: the lymphocyte function-associated antigen (LFA-1), the C3bi

- complement receptor (OKM1/Mac-1), and the p150,95 molecule. *J. Exp. Med.* **158**, 1785-1803
78. Schlesinger, L.S. (1993). Macrophage phagocytosis of virulent but not attenuated strains of *Mycobacterium tuberculosis* is mediated by mannose receptors in addition to complement receptors. *J. Immunol.* **150**, 2920-2930
79. Schuller, S., Neefjes, J., Ottenhoff, T., Thole, J. and Young, D. (2001). Coronin is involved in uptake of *Mycobacterium bovis* BCG in human macrophages but not in phagosome maintenance. *Cell Microbiol.* **3**, 785-793
80. Simonsen, A., Lippe, R., Christoforidis, S., Gaullier, J.M., Brech, A., Callaghan, J., Toh, B.H., Murphy, C., Zerial, M. and Stenmark, H. (1998). EEA1 links PI(3)K function to rab5 regulation of endosome fusion. *Nature* **394**, 494-498
81. Simonsen, A., Gaullier, J.M., D'Arrigo, A., and Stenmark, H. (1999). The rab5 effector interacts directly with Syntaxin 6. *J. Biol. Chem.* **274**, 28857-28860
82. Smith, P.K., Krohn, R.I., Hermanson, G.T., Mallia, A.K., Gartner, F.H., Provenzano, M.D., Fujimoto, E.K., Goeke, N.M., Olson, B.J., klenk, D.C. (1985). Measurement of protein using bicinchoninic acid. *J Anal. Biochem.* **150**, 76-85
83. Springer, T.A. (1997). Folding of the N-terminal, ligand-binding region of integrin α -subunits into a β -propeller domain. *Proc. Natl. Acad. Sci. USA.* **94**, 65-72
84. Stenmark, H., Aasland, R., Toh, B.H. and D'Arrigo, A. (1996). Endosomal Localization of the Autoantigen EEA1 is Mediated by a Zinc-binding FYVE finger. *J. Biol. Chem.* **271**, 24048-24054
85. Sturgill-Koszycki, S., Schlesinger, P.H., Chakraborty, P., Haddix, P.L., Collins, H.L., Fok, A.K., Allen, R.D., Gluck, S.L., Heuser, J. and Russel, D.G. (1994). Lack of

- Acidification in *Mycobacterium* Phagosomes Produced by Exclusion of the Vesicular Proton-ATPase. *Science* **263**, 678-680
86. Taunton, J., Rowning, B.A., Coughlin, M.L., Wu, M., Moon, R.T., Mitchison, T.J. and Larabell, C.A. (2000). Actin-dependent propulsion of endosomes and Lysosomes by recruitment of N-WASP. *J. Cell Biol.* **148**, 519-530
87. Thilo, L. (1983). Labeling of Plasma Membrane Glycoconjugates by Terminal Glycosylation (Galactosyltransferase and Glycosidase). *Methods in Enzymology* **98**, 415-421
88. Ullrich, H.J., Beatty, W.L. and Russel, D.G. (1999). Direct delivery of pro-cathepsin D to phagosomes: implications for phagosome biogenesis and parasitism by *Mycobacterium*. *Eur. J. Cell Biol.* **78**, 739-748
89. Van Gelder, R.N., Von Zastrow, M.E., Yool, A., Dement, W.C., Barchas, J.D., and Eberwine, J.H. (1990). Amplified RNA Synthesized from Limited Quantities of Heterogeneous cDNA. *Proc. Natl. Acad. Sci. USA.* **87**, 1663-1667
90. Velasco-Velázquez, M.A., Barrera, D., González-Arenas, A., Rosales, C., and Agramonte-Hevia, J. (2003). Macrophage-*Mycobacterium tuberculosis* interactions: role of complement receptor 3. *Microbial Pathogenesis* **35**, 125-131
91. Via, L.E., Deretic, D., Ulmer, R.J., Hibler, N.S., Huber, L.A. and Deretic, V. (1997). Arrest of Mycobacterial Phagosome Maturation Is Caused by a Block in Vesicle Fusion between Stages Controlled by rab5 and rab7. *J. Biol. Chem.* **272**, 13326-13331
92. Vieira, O.V., Betelho, R.J., Rameh, L., Brachmann, S.M., Matsuo, T., Davidson, H.W., Schreiber, A., Backer, J.M., Cantley, L.C., Grinstein, S. (2001). Distinct roles

- of class I and class III phosphatidylinositol in phagosome formation and maturation. *J. Cell Biol.* **155**, 19-25
93. Vitelli, R., Santillo, M., Lattero, D., Chiariello, M., Bifulco, M., Bruni, C.B. and Bucci, C. (1997). Role of the small GTPase Rab7 in the late endocytic pathway. *J. Biol. Chem.* **272**, 4391-4397
94. Wiechelman, K.J., Braun, R.D., and Fitzpatrick, J.D. (1988). Investigation of the bicinchoninic acid protein assay: Identification of the groups responsible for the color formation. *J. Anal. Biochem.* **175**, 231-237
95. Wright, S.D., Rao, P.E., Van Voorhis, W.C., Craigmyle, L.S., Iida, K., Talle, M.A., Westberg, E.F., Goldstein, G., and Silverstein, S.C., (1983). Identification of the C3bi receptor of the human monocytes and macrophages by using monoclonal antibodies. *Proc. Natl. Acad. Sci. USA.* **80**, 5699-5703
96. Wright, S.D., Levin, S.M., Jong, M.T.C., Chad, Z., and Kabbash, L.G. (1989). CR3 (CD11b/CD18) expresses one binding site for Arg-Gly-Asp-containing peptides and a second site for bacterial lipopolysaccharide. *J. Exp. Med.* **169**, 175-183
97. Xiong, Y., Chen, J., and Zhang, L. (2003). Modulation of CD11b/CD18 Adhesive Activity by its Extracellular, Membrane-Proximal Regions. *J. Immunol.* **171**, 1042-1050
98. Xu, S., Cooper, A., Sturgill-Koszycki, S., van Heyningen, T., Chatterjee, D., Orme, I., Allen, P. (1994). Intracellular trafficking in *Mycobacterium tuberculosis* and *Mycobacterium avium*-infected macrophages. *J. Immunol.* **153**, 2568-2578

99. Zhang, L., and Plow, E.F. (1996). Overlapping, but Not Identical, Sites Are Involved in the Recognition of C3bi, Neutrophil Inhibitory Factor, and Adhesive Ligands by the $\alpha_M\beta_2$ Integrin. *J. Biol. Chem.* **271**, 18211-18216
100. Zhou, M. and Brown, E. (1994). CR3 (Mac-1, $\alpha_M\beta_2$, CD11b/CD18) and Fc γ RIII Cooperate in Generation of a Neutrophil Respiratory Burst: Requirement for Fc γ RII and Tyrosine Phosphorylation. *J. Cell Biol.* **125**, 1407-1416

Chapter 4: MATERIALS AND METHODS

4.1 Harvesting of mouse bone marrow-derived macrophages and cell culturing

Mouse bone marrow-derived macrophages were obtained by the method described by Frehel *et al.*, 1986. Six-eight-weeks old mice were sacrificed by cervical dislocation and the femurs were removed from the hind legs. After scraping off the tissue around the bones, both ends of each bone were cut with a scalpel blade. The marrow (stem cells) was flushed out from the bones by gently passing RPMI HEPES [RPMI 1640 powder was obtained from Highveld Biological (PTY) Ltd, Republic of South Africa; HEPES(2-[4-(2-Hydroxyethyl)-1-piperazinyl]-ethansulfoni acid) from Merck, Darmstadt, Germany] medium through the bones with a syringe. The cells were resuspended in an appropriate volume of RPMI HCO₃⁻ medium (0.04 mM NaHCO₃, Merck, Germany) supplemented with 10% heat-inactivated foetal calf serum (Highveld Biological (PTY) LTD, Republic of South Africa) and 10% conditioned medium (source of colony stimulating factor (CSF) prepared from L929 fibroblast (a kind donation from Dr. Jacob Muazzam, Division of Immunology, University of Cape Town Medical School, RSA). Usually 1-2 X 10⁶ cells were seeded in each lumox dish (Greiner bio-one, Germany). The dishes were incubated at 37°C in a 5% CO₂ incubator for five days to allow for differentiation of the stem cells into macrophages and for adherence of the cells to the dishes. Adherent cells were rinsed twice with RPMI HEPES medium and refed with growth medium after every 48 hours. Once differentiated, these macrophages can be kept in culture for close two months without losing their capacity to internalise endocytic markers, particles or microorganisms (Frehel *et al.*, 1986).

4.2 Culturing and storage of *Mycobacterium avium*

Mycobacterium avium isolated from mouse liver of C57Bl/6 mice infected 6-8 weeks previously were kindly donated by Dr. Chantal de Chastellier (Centre d'Immunologie de Marseille, Luminy, Marseille) and Dr. Georg Plum, University of Cologne, Germany (de Chastellier *et al.*, 1995, de Chastellier and Thilo, 2002). The bacteria were plated on freshly prepared Middlebrook 7H10 agar (Becton Dickinson, Maryland USA) plates. The plates were incubated at 37°C for 7-10 days after which colonies had formed. The colonies were scraped using a glass or plastic loop under sterile conditions. These were mixed properly, aliquoted into culture vials in an appropriate volume, and stored at -70°C. The bacterial titre of the aliquots was determined by serially diluting a single vial with 7H9 agar solution and plating on Middlebrook 7H10 agar plates. The plates were incubated at 37°C until single and easily detectable colonies were formed. The colonies from an appropriate dilution were counted and the concentration of the bacteria was determined using the appropriate dilution factor.

4.3 Infection of macrophages with *M. avium*

Mouse bone marrow-derived macrophages were infected as described by Frehel *et al.*, 1986. After 7 days of growth, the cell count was determined using the Neubauer counting chamber (Superior, Germany). Using an infection ratio of 1:20 macrophage/bacteria, the frozen *Mycobacterium avium* stocks were thawed, vortexed gently, and adjusted to the desired titre with complete cell culture medium. The bacteria were added to the cells and incubated for 4 hours at 37°C in a 5% CO₂ incubator. Non-ingested bacteria were removed by washing the cells four times with RPMI HEPES. The

cells were further incubated in complete culture medium for up to 7 days with the medium being changed after every 2 days.

4.4 Preparation of *M. avium*-infected cells for electron microscopy

The cells were processed for electron microscopy according to de Chastellier *et al* 1995. Seven days after infection with *M. avium*, mouse macrophages were fixed with 2.5% glutaraldehyde (Sigma-Aldrich, St. Louis, USA) in 0.1M sodium cacodylate buffer pH 7.2 containing 5mM CaCl₂, 5mM MgCl₂ and 0.1M sucrose for 1 hour at room temperature. This was followed by two washes with sucrose-containing cacodylate buffer for 15minutes intervals. The cells were then fixed with 1% Osmium tetroxide (OsO₄) [Sigma-Aldrich, USA] in sodium cacodylate buffer without sucrose for 1 hour at room temperature. The cells were further rinsed twice with sodium cacodylate without sucrose for 30 seconds duration. With the aid of a rubber policeman, the cells were scrapped off from the culture dishes in sodium cacodylate buffer and treated for 1 hour at room temperature with 1% Uranyl acetate in Veronal buffer. The samples were dehydrated in acetone and embedded in Epon. Thin sections were stained with 1% Uranyl acetate in distilled H₂O and then lead citrate.

4.5 Labelling and isolation of plasma membrane glycoproteins

Labelling of plasma membrane glycoproteins of both uninfected and *M. avium*-infected macrophages was performed by the method of exo-galactosylation described by Thilo, 1983 (as shown schematically in Diag. 2). The entire labelling experiment was carried out on ice to stop membrane internalisation. Briefly, culture medium was

removed and the cells were washed twice with HEPES saline (10mM HEPES, 140mM NaCl, pH 7.4; Merck, Germany). The different cell types were pre-treated on ice with 0.2 Units of a cocktail of β -galactosidase and β -neuraminidase for 10 minutes to remove N-terminal neuraminic acid and galactose present on sugar chains that are attached to plasma-membrane proteins. The cells were washed twice with ice-cold HEPES saline pH 7.4 to stop the action of the enzymes. Depending on the nature of the experiment, *M. avium*-infected and uninfected macrophages were labelled for 30 minutes on ice with [14 C]-UDP-galactose, a lithium salt; and [3 H]-UDP-galactose, an ammonium salt (Amersham Biosciences, United Kingdom) respectively, or with the same isotope. The labelling mix consisted of 5 μ Ci of each of the radioisotope, 0.5units of the labelling enzyme galactosyltransferase (Sigma-Aldrich, St Louis, USA), 5mM MnCl₂ (supplied by B & M Scientific, Cape Town, South Africa) and HEPES saline pH 7.4. The cells were washed four times with HEPES saline to remove unbound label. Labelled cells were washed briefly in homogenisation buffer (0.25M sucrose, 2mM EDTA, 10mM HEPES, pH 7.4). The different batches of cells were scraped separately with a rubber policeman in about 300 μ l of homogenisation buffer (HB) supplemented with protease inhibitors cocktail (Sigma-Aldrich, St Louis, USA) at 1mM final concentration. The cells were homogenised by making 8-10 passages through a ball bearing in a cell cracker. Postnuclear supernatant (PNS) from each cell type was obtained by centrifuging the homogenate at 2000rpm for 12 minutes. These were layered on appropriate volumes of separate 27% Percoll (Sigma-Aldrich, USA) gradient column [made using 27% Percoll and 73% HB₂₇ (340mM sucrose, 2.7mM EDTA, 13.7mM HEPES)] in Polyallomer Beckman centrifuge tubes (Beckman Instruments Inc. California, USA). A volume of

0.5 millilitre (ml) of 80% sucrose was placed at the bottom of the column to prevent cushion during centrifugation. These were centrifuged in a Beckman ultracentrifuge using a SW40 swing-out rotor at 15000rpm for 90 minutes at 4°C. The tubes were then pierced with a syringe connected to a LKB2112 RediRac fraction collector (LKB-Produkter AB, Bromma, Sweden). Different cell organelles were collected into different fraction collection tubes. The cell fractionation machine was programmed for 10 drops (0.5ml) per tube. An aliquot of 20µl was taken from each fraction for each cell type for β-counting in a liquid-scintillation analyser (Packard Instrument Company, Inc. Illinois, USA). For each cell type, fractions containing labelled membrane proteins were pooled out and washed in homogenisation buffer (HB) by centrifuging at 100000g for 2 hours at 4°C in order to remove excess Percoll. The membrane proteins were further sonicated in 0.5M KCl in HB for 30X5seconds pulses with a sonicator (Cell disruptor model W-10, Scientific Associates, Tokai, South Africa) and centrifuged at 100000g in a fixed angled 70.1 Ti rotor (Beckman Instruments, Inc. USA). The membrane pellets were further centrifuged in an airfuge machine (Beckman Instruments, Inc. USA) at 28 psi (pressure per square inches) for 30minutes at 4°C.

4.5.1 Protein quantification assays

The amount of protein present in each sample was quantified by using either Bio-rad or Bicinchoninic acid (BCA) protein assays.

4.5.1.1 Bio-rad protein assay

This was originally described by Bradford, 1976. It is based on the principle that the binding of Coomassie brilliant blue G-250 (red) to protein to form a protein-dye complex

(blue) leads to a change in the absorption maximum of the dye from 465nm to 595nm. The absorbance being read by the spectrophotometer corresponds to that at 595nm. The reagents present in the Bio-rad protein assay solution have a final concentration of 0.01% (w/v) Coomassie Brilliant Blue G-250, 4.7% (w/v) ethanol and 8.5% (w/v) phosphoric acid. A volume of 200 μ l of the Bio-rad solution was added to an appropriate volume of distilled H₂O in an eppendorf tube and vortexed briefly. A few micro litres (μ l) of the protein solution were added to the mixture. The mixture was vortexed briefly and left to stand at room temperature for over 5minutes prior to reading in the spectrophotometer. The binding of the protein to the dye is completed after 2minutes and the complex (protein-dye) can remain in solution up to an hour after which it starts precipitating out of solution (Bradford, 1976). The mixture was transferred into a glass cuvette and the absorbance was read at 595nm in a spectrophotometer (Hitachi U-2000 spectrophotometer, LabX, New Jersey, USA). The amount of protein present per μ l of sample was determined by interpolating to a standard curve generated from a protein, bovine serum albumin (BSA), of known concentration.

4.5.1.2 Bicinchoninic acid (BCA) protein assay

The BCA protein assay was described by Smith *et al.*, 1985. The technique is based on the ability of bicinchoninic acid to form an intense purple complex with cuprous ion (Cu⁺¹) in an alkaline environment. The cuprous ion is formed from the reduction of cupric sulphate (Cu²⁺) by protein. The protein structure, number of peptides and the presence of four particular amino acids; cysteine, cystine, tryptophan and tyrosine have been reported to be responsible for the colour formation with bicinchoninic acid

(Wiechelman *et al.*, 1988). Briefly, a working reagent was prepared by mixing 50 parts of reagent A (containing sodium carbonate, sodium bicarbonate, bicinchoninic acid and sodium tartrate in 0.1M sodium hydroxide) with one part of reagent B (containing 4% cupric sulphate). A volume of 5 μ l of the diluted standard protein (Bovine serum albumin) and the unknown protein samples was aliquoted in duplicates into 96 wells ELISA plate (Greiner bio-one, Germany). A hundred microlitres of working reagent was added to each sample and mixed properly. The plate was covered with aluminium foil and incubated at 37°C for 30 minutes. It was then cooled to room temperature and the absorbance was measured at 560nm on an ELISA plate reader (Labsystem Multiskan MS, type 352, made in Finland by Labsystem). The protein concentration of the unknown samples was determined by interpolation to a standard curve generated from plotting the absorbance of diluted standard protein against known protein concentrations.

4.6 Protein electrophoresis

4.6.1 Gradient SDS-PAGE for determination of radioactivity profiles of labelled plasma membrane proteins

4.6.1.1 Preparation and pouring of an 8%-15% gradient SDS-PAGE

Separately, an 8% and a 15% running gel solutions were prepared from 4X lower gel buffer (1.5M Tris, 0.4% sodium dodecyl sulphate, pH 8.8), acrylamide (30% acrylamide, 0.8% bisacrylamide and distilled H₂O, filtered through Whatman fluted paper and stored in dark bottle at 4°C) and made up to the required volume with distilled H₂O. An additional 2.5M sucrose (80%) was added to the 15% running gel solution. Sodium

dodecyl sulphate was purchased from BDH Laboratory Supplies, Poole, England. Acrylamide, bisacrylamide, and sucrose were purchased from Merck Chemicals, Germany.

After degassing, Temed (N, N, N, N tetramethylethylenediamin) [Merck Chemicals, Germany] and 10% ammonium persulphate were added to each gel solution and mixed properly. The solutions were poured into separate columns of a gradient mixer that had been connected to a peristaltic pump that was in turn connected to a thin tube placed between two assembled gel plates. With the aid of the pump, the resultant mixed gel solution was poured gently into the plates and immediately overlaid with an overlay buffer that was made up from distilled H₂O and 4X lower gel buffer. The gel was left to stand overnight at room temperature to allow for better polymerization.

4.6.1.2 Preparation and pouring of the stacking gel

The stacking gel was prepared from 4X upper gel buffer (0.5M Tris, 0.4% sodium dodecyl sulphate and distilled H₂O, pH 6.3), acrylamide. TEMED and 10% ammonium persulphate were added and mixed properly. The overlay buffer was replaced by the stacking gel solution and an appropriate comb was inserted into the gel immediately. This was left to polymerise for a few minutes.

4.6.1.3 Loading and separation of proteins

The assembled gel plates containing the polymerised running gel were mounted onto the gel tank and sufficient running buffer (0.25mM Tris, 192mM glycine, 0.1% sodium dodecyl sulphate, H₂O, pH 8.3) was poured into the upper and lower parts of the gel tank. The gel tank was connected to an electrophoresis power supply (EPS 500/400, Pharmacia Fine Chemicals, Hoefer Scientific Instruments, San Francisco, USA) by two electrodes.

The comb was gently pulled out from the stacking gel and the wells were washed with running buffer to remove any gel pieces that may disturb loading and separation of the samples.

Depending on the labelling intensity, ^{14}C - and ^3H -labelled plasma membrane proteins from *M. avium*-infected and non-infected macrophages, respectively, or vice versa, were mixed together. The mixture was resuspended in an appropriate volume of reducing sample buffer (10% glycerol, 0.25M sucrose, 2.3% sodium dodecyl sulphate, 8.3% of 4X upper gel buffer, a crystal of bromophenol blue, H_2O and 5% β -mercaptoethanol) and boiled for 3-5 minutes. The protein mixture was loaded into the well with an Hamilton Microlitre Syringe (HAMILTON, Hamilton Bonaduz AG, ch-7402 Bonaduz, Switzerland). Sample buffer was also loaded into unused wells in order to diffuse the effect of the current across the entire gel surface. The proteins were separated at a constant current of 20mA for approximately 16hours.

4.6.2 Lined SDS-PAGE for Western Blotting

For most Western Blot analysis, the Mini-PROTEAN II Electrophoresis Cell system (Bio-rad Laboratories, Inc., USA) was used for casting of the gel and running of samples. The system is composed of a lower buffer chamber and a lid, a casting stand, an inner cooling core, two glass plates, spacers and sandwich clamp assemblies. The system was assembled according to the manufacturer's instruction manual. An 8% SDS-PAGE was prepared and poured as in 4.5.1.2. The stacking gel was prepared as in 4.5.1.3. An appropriate comb was inserted immediately and the stacking gel was allowed to set for about 15 minutes.

For Western blot analysis, suitably determined amounts of 2 μ g and 4 μ g of membrane proteins from *M. avium*-infected and non-infected macrophages were made up separately in an appropriate volume of non-reduced sample buffer. (10% glycerol, 1.2% SDS (w/v), a crystal of bromophenol blue, 8.3% of upper gel buffer, and distilled H₂O). The samples and a Prestained Precision Plus protein dual color molecular-weight marker (Bio-rad Laboratories, Inc., USA) were loaded into separate wells and electrophoresed for 45 minutes at 60mA, with a constant voltage setting of 200volts.

4.6.2.1 Western blotting

After electrophoresis, the gel was rinsed briefly with distilled H₂O and equilibrated in protein transfer buffer (19.8mM Tris and 14.9mM Glycine) for 15-20 minutes. A piece of Hybond™ ECL™ nitrocellulose membrane (Amersham Pharmacia Biotech, UK Limited, Buckinghamshire, England) of an appropriate size was pre-wet with distilled H₂O and also equilibrated in the protein transfer buffer for not less than 15 minutes. Together with 2 pieces of pre-wet Whatman 3MM paper and two sponges, the gel was sandwiched in an assembly cassette and connected according to the manufacturer's instruction manual. Protein transfer was done for 1-2 hours at 100volts.

Following blotting, the nitrocellulose membrane was rinsed briefly with tris buffered saline (10mM Tris, 150mM NaCl, pH 7.6) and then blocked in 5% Milk in tris buffered saline with 0.1% Tween 20 (TBS-T) [Merck Chemicals, Germany] for 1 hour at room temperature, with shaking. The membrane was further incubated in rat anti-mouse anti-integrin- β_2 monoclonal antibody (Beckton Dickinson, USA) at a dilution of 1 in 10000, made up in 5% Milk in tris buffered saline with 0.1% Tween 20 (TBS-T), for 1 hour at room temperature. The membrane was rinsed twice briefly with TBS-T solution and then

for 15 minutes on a shaker. This was followed by two subsequent washes of 5 minutes each. The nitrocellulose membrane was then incubated in HRP-conjugated rabbit anti-rat monoclonal antibody (Amersham Bioscience UK Limited, England) for 1 hour at room temperature. It was rinsed twice briefly with TBS-T and then washed for 15 minutes on a shaker, followed by two washes for 5 minutes each. The membrane was allowed to air-dry and later taken to the dark room for exposure to X-ray film. While in the dark room, with only the safe light on, the nitrocellulose membrane was incubated into a mixture of ECL detection reagents 1 and 2 (equal volumes) [Amersham Bioscience] for 2 minutes. The membrane was drain rapidly and placed between folded overhead transparencies fixed to a cassette. It was then exposed to an X-ray film for time intervals that had been previously determined for which the signal is still strong. The film was immediately placed in a film developer for 2 minutes, rinsed with tap water for 1 minutes and placed into a fixer for 2 minutes. It was further rinsed with tap water and allowed to air-dry

4.7 Visualisation of protein bands on SDS-PAGE by Coomassie Brilliant Blue staining protocol

At the end of electrophoresis, protein bands were visualised using Coomassie brilliant blue staining protocol. The gel was placed into a stain solution (46% Methanol, 8% Acetic acid, and 0.1% Coomassie Brilliant Blue R (Sigma)) for 30 minutes with shaking. The stain solution was removed and the gel was rinsed briefly with about 50ml of destain solution (20% Methanol and 8% Acetic acid). An appropriate volume of destain solution was added to the gel and shaken for 30-60 minutes. The destain solution was replaced and shaken for another 30-60 minutes. The destaining was repeated until the

protein lanes became visible. The solution was replaced with an appropriate volume of gel drying solution (3% Acetic acid and 2% Glycerol) and the gel was shaken for 30 minutes. This was repeated and the gel was later dried in a slap gel drier (Hoefer Scientific Instruments, USA).

4.8 Autoradiography

Depending on the nature of the experiment, the dried SDS-PAGE, containing ^{14}C -labelled membrane proteins, was exposed to a Cyclone phosphor-imager screen in a dark Lead box for over 48 hours to allow for enough ^{14}C -beta emissions to be imprinted on the screen. The screen was then loaded into a Cyclone phosphor-imager machine (Packard Bioscience, IL, USA). Molecular-weight markers were traced with a ^{14}C -labelled ink.

4.9 Trypsin ingel digestion

The lane that contained mixed ^{14}C - and ^3H -labelled membrane proteins from *M. avium*-infected and uninfected mouse macrophages, respectively, was analyzed by trypsin digestion. Trypsin catalyses the cleavage of proteins on the carboxy sides of lysine and arginine residues thereby producing peptides which diffuse easily from the gel. The lane was divided into 2.5mm wide slices. The slices were rehydrated twice in 0.05% trypsin at 37°C for 4 hours per round. The digestion product from each slice was counted in a liquid-scintillation counter. The amount of radioactivity (dpm) obtained per slice was plotted against slice number.

4.10 RNA isolation from uninfected and *M. avium*-infected mouse bone marrow-derived macrophages

RNA was isolated using the Trizol reagent (Invitrogen, California, USA). After seven days of infection with *M. avium* or not, macrophages were rinsed twice with buffered phosphate saline solution (137mM NaCl, 10mM phosphate, 2.7mM KCl, pH 7.4). Each millilitre of Trizol (Invitrogen Corporation, USA) was used to scrape about 7-10 million non-infected and *M. avium*-infected cells separately from two to three 60mm culture dishes (Greiner bio-one, Germany) with the aid of a rubber policeman. Each batch of cells was mixed well to ensure proper cell lysis. A volume of 0.2millilitre of chloroform was added to each sample in an eppendorf tube. The eppendorf tubes were inverted by hand for 15 seconds and left on ice for 10 minutes. The samples were then centrifuged at 12000g for 15minutes at 4°C. The aqueous phase from each tube was transferred into a new eppendorf tube. A volume of 0.5millilitre of isopropanol was added to each aqueous phase and precipitated overnight or for 1 hour at -20°C. The samples were then centrifuged at 8000rpm for 30 minutes at 4°C. The supernatants were discarded and each pellet was resuspended in 1millilitre of 75% ethanol. These were centrifuged at 8000rpm for 30minutes at 4°C. The supernatants were poured off and the pellets were air-dried on the bench. The pellets were further resuspended separately in 200µl of diethylpyrocarbonate (DEPC)-treated H₂O and transferred to new tubes. Volumes of 200µl of isopropanol and 20µl of 3M sodium acetate were added to each sample and precipitated at -20°C for 1 hour. The samples were further centrifuged at 15000rpm for 30 minutes at 4°C. The supernatants were poured off and the pellets were washed with 70% ethanol by centrifuging at 15000rpm for a further 30 minutes at 4°C. The pellets

were air-dried on the bench and resuspended in an appropriate volume of diethylpyrocarbonate (DEPC)-treated H₂O.

4.10.1 Determination of RNA concentration

The amount of RNA present in each sample was determined by reading the absorbance of each diluted sample at 260nm. Briefly, two microlitre from each RNA sample (from *M. avium*-infected and uninfected macrophages) was added to 500µl of distilled H₂O in separate eppendorf tubes, giving a 1 in 250 dilution. Each sample was mixed well and pipetted into a glass curvette. The absorbance reading for each sample was obtained at a wavelength of 260nm using a Beckman DU-600 spectrophotometer (Beckman Instruments Inc, USA). The concentration, in microgram per microlilitre, was calculated by multiplying each absorbance reading by 10.

4.10.2 Checking the integrity of the RNA obtained

The quality of RNA obtained was checked by analyzing 2µg and 4µg of RNA from each sample on a 1.5% formaldehyde agarose gel. A mass of 1.5g of agarose was dissolved in 10% MOPS (3-Morpholinopropanesulfonic acid) buffer [0.2M MOPS, 0.005M sodium acetate, 0.01M EDTA] by warming the agarose solution for few minutes in a microwave. Once dissolved and cooled, formaldehyde and ethidium bromide were added, under a fume cupboard, at final concentrations of 2% and 0.5µg/ml respectively. The gel was poured into a casting chamber containing an appropriate comb and allowed to set for close to 30 minutes. The gel was submerged in TBE buffer (108g tris, 55g boric acid, 7.4g EDTA). Two and four microgram of RNA from each sample was made up in RNA loading buffer (48% formamide, 10% MOPS buffer, 17% formaldehyde, 5.3% glycerol, and 5.3% bromophenol blue; stored at -20°C) and loaded in separate wells. The

samples were electrophoresed using an Amersham power pack at 80volts for 30 minutes. After separation, the gel was removed and photographed with a UV gel doc machine.

4.10.3 Single strand (cDNA) synthesis

Single strand DNA (cDNA) was synthesized from RNA using a modified method originally described by Van Gelder *et al.*, 1990, with slight modification. An amount of 4µg of RNA from *M. avium*-infected and non-infected macrophages was made up to a final volume of 8µl with ultrapure H₂O in separate eppendorf tubes. One microlitre of qRT-PCR Oligo dT primer (Invitrogen) was added to each sample and incubated at 70°C for 10 minutes in a heating block. After heating, the samples were span briefly and left on ice. A mixture composed of 8µl of 5X first strand buffer, 4µl of 0.1M DTT, 4µl of 10mM dNTP, 2µl of RNAsin (RNAase inhibitor) and 4µl of Superscript II (reverse transcriptase enzyme) [all from Invitrogen] was prepared and 11µl was added to each sample to give a final volume of 20µl. The samples were mixed properly and incubated in a water bath set at 42°C for 2 hours. They were span briefly and placed on ice. A volume of 20µl of 0.1% DEPC-treated water was added to each sample to bring the concentration to 0.1µg/µl. Ten microlitre aliquots were prepared and stored at -70°C until when used.

4.11 Bioinformatics

The mouse gene transcripts for integrin- α_M and - β_2 were obtained from the ensembl website (<http://www.ensembl.org/index.html>) and primer sets for both integrin- α_M and integrin- β_2 were designed using Primer3 software that is freely available on the internet. Specifically, primers were designed across the intron-exon boundaries between the preceding and proceeding exon, of exon 5 and 29 for integrin- β_2 and - α_M , respectively. A

list of possible primer sets was obtained for each gene and the one with the highest percentage identity was chosen for synthesis. Primer length of 20 base pairs was chosen. A nucleotide-nucleotide blast search was performed on the NCBI website (<http://www.ncbi.nih.gov>) using any of the primer sequences obtained for each gene from Primer3 software in order to ensure that the primer set was specific for amplification of either mouse integrin- β_2 or $-\alpha_M$ gene.

4.12 Quantitative Real time Reverse Transcription Polymerase Chain Reaction (qRT-PCR)

4.12.1 Synthesis of primers

A pair of primers for exons 5 and 29 for integrins- β_2 and $-\alpha_M$ genes, respectively, was designed as described in 4.11 above. The nucleotide sequences for each primer pair were sent to the department of Molecular and Cell Biology at the University of Cape Town, South Africa, for synthesis using the Oligo 1000M DNA synthesizer (Beckman Instruments Inc.USA). The primers were synthesized at a stock concentration of 30nM. The sequences were as follows; integrin- β_2 forward primer: 5' CTGACCCACCTGACTGACCT 3', reverse primer: 5' GGGGTCACATCTGCTTGATT 3'; integrin- α_M forward primer: 5' GATGCAGCTCACAGCACAGT 3', reverse primer: 5' CCTAAGGAGAGACCCCAAC 3'.

4.12.2 Real time Reverse transcriptase polymerase chain reaction (Real time RT-PCR) - cDNA amplification

The polymerase chain reaction was performed using the LightCycler FastStart DNA Master SYBR Green I reaction mix with the LightCycler instrument (Roche Diagnostic).

For each sample, the PCR mix for the exon of interest of each gene was made up using 13.6 μ l of H₂O (PCR grade), 2.4 μ l of MgCl₂ (4mM), 1 μ l of each of the primers (100ng/ μ l), and 1 μ l of the LightCycler Faststart SYBR Green I. The PCR mix for the control gene, glutaraldehyde phospho dehydrogenase (GAPDH), was also prepared using its set of primers. Separately, the reaction mixtures were mixed gently and transferred into pre-cooled capillary tubes in adapters. A volume of 1 μ l of cDNA template prepared from *M. avium*-infected and non-infected macrophages was added to the capillary tubes for each gene. Each tube was sealed with a stopper and the adapters containing the tubes were placed into a standard bench top microcentrifuge, and centrifuged at 700g for 5 seconds. The capillaries were placed into the rotor of the LightCycler instrument. The polymerase chain reaction (PCR) conditions were set as follows: one cycle of activation at 95°C for 10 minutes followed by 45 cycles of amplification of 10 seconds at 95°C, 5 seconds at 55°C, 10 seconds at 72°C, one cycle of melting for 15 seconds at 65°C and finally a cooling cycle for 30 seconds at 40°C. At the end of the reaction, melting curves, and curves showing the rate of product formation were printed. The levels of expression of each of the genes per sample were calculated using the $2^{-\Delta\Delta C_T}$ method described by Livak and Schmittgen, (2001). GAPDH C_T values were used as a control.

4.12.3 DNA electrophoresis of PCR products

The specificity of the polymerase chain reactions for amplification of exons 5 and 29 for integrin- β_2 and integrin- α_M , respectively, was checked by analysing the PCR products on a 2% agarose gel. The gel was made by first warming 2grams of agarose powder in tris borate EDTA buffer in a microwave for a few minutes. Once dissolved and cooled, ethidium bromide was added under a fume cupboard to a final concentration of 2.5 μ g/ml.

The gel was poured onto a casting chamber containing an appropriate comb. After setting, the gel was submerged into tris borate EDTA (TBE) buffer in a DNA electrophoresis chamber. Separately, 3 μ l of 6X DNA loading buffer (Fermentas, Fermentas Inc., Hanover, Maryland, USA) was added to 15 μ l of each PCR product in a reswelling chamber. The samples were mixed well and loaded into separate wells. A volume of 5 μ l of 50kilobase pairs marker was loaded into a separate well. The samples were electrophoresed at 80volts for one to two hours using an electrophoresis power pack (Amersham). After electrophoresis, gel pictures were taken using UV gel doc machine.

4.13 Immunofluorescence

4.13.1 Surface staining of integrin β_2 and α_M on *M. avium*-infected and non-infected macrophages

Cell-surface immunofluorescence studies were done according to Maske *et al*, 2003. Seven days post-infection, infected and non-infected macrophages at the same stage of growth were blocked with 1% bovine serum albumin (BSA) and rat anti-Fc γ RII/III blocking monoclonal antibody (BD Bioscience, USA) [1/100 dilution] for 30 minutes at room temperature. The bottoms of the Petriperm dishes separately containing *M. avium*-infected and non-infected cells were cut out and divided into sections. For each cell type, different sections were stained with either FITC-conjugated rat anti-mouse anti-integrin- β_2 [C71/16] or Alexa 488-conjugated rat anti-mouse anti-integrin- α_M [M1/70] monoclonal antibodies (BD Bioscience) at 4°C for 1hour at a dilution of 1/100. All antibody dilutions were made in 1% BSA HEPES saline solution. The cells were washed twice for 10 minutes each with cold HEPES saline pH 7.4 and then fixed with 4%

paraformaldehyde (PFA) for 10 minutes at room temperature. After fixation, the cells were washed three times for 10 minutes each with HEPES saline. The nuclei were stained with 4', 6-Diamidino-2-phenylindole (DAPI) for 10 minutes at room temperature and were washed with cold HEPES saline for 10 minutes. As a control, after the blocking step, the cells were processed normally but without either antibody staining. The films containing the cells were placed on microscope slides. A drop of mowiol, containing an anti-fading agent N-propyl galate (Sigma-Aldrich, USA), was placed on the cells and then covered with a glass microscope cover slip. The cells were then viewed using Carl Zeiss Axioskop 40 fluorescence microscope fitted with AxioCam MRm camera at a X20 or X40 magnification.

4.13.2 Intracellular staining of integrin- β_2 and $-\alpha_M$ in *M. avium*-infected and uninfected mouse bone marrow-derived macrophages

Intracellular staining of integrin- β_2 and $-\alpha_M$ was done according to the protocol described by Christopher P. Maske and David J. Vaux under Immunofluorescence technique in *Advance Methods: cell proliferation and Apoptosis*. At day 7 after infection, *M. avium*-infected and uninfected mouse macrophages were rinsed briefly with HEPES saline and then fixed with 4% paraformaldehyde in PBS for 30 minutes at room temperature. The cells were washed trice for 5 minutes each with HEPES saline and then permeabilised with 0.5% Triton-X-100 in HEPES saline for 5 minutes at room temperature. Free aldehyde groups were quenched by treating the cells with 0.1M glycine in HEPES saline for 5 minutes. Non-specific sites were blocked with 1% BSA in HEPES saline for 30 minutes at room temperature. Both cell types were then stained with either FITC-conjugated anti-integrin- β_2 (1/100 dilution) [C71/16] or Alexa 488-conjugated

anti-integrin- α_M (1/100 dilution) [M1/70] monoclonal antibodies for 45 minutes at room temperature. All antibody dilutions were done in 1% BSA HEPES saline. Unbound antibodies were removed by washing three times with buffer for 5 minutes each. The nuclei were stained with DAPI at room temperature and the cells were mounted using mowiol. Images were taken using the Carl Zeiss fluorescence microscope fitted with AxioCam MRm camera at a X40 magnification.

4.14 Co-immunoprecipitation of ^{14}C -labelled $\alpha_M\beta_2$

At day 7 post-infection, two sets of three dishes each, one set containing *M. avium*-infected macrophages and the other set containing non-infected macrophages were rinsed twice with HEPES saline pH 7.4. Both batches of cells were pretreated with 0.2 units of β -galactosidase for 10 minutes and then labelled radioactively with ^{14}C -galactose for 30 minutes on ice. Unbound label was removed by washing the cells four times with HEPES saline. The cells were further rinsed once with Co-immunoprecipitation buffer (20mM Tris, 150mM NaCl, pH 7.4, 2mM CaCl_2) and lysed separately with lysis buffer (20mM Tris, 150mM NaCl, 2mM CaCl_2 , 1% Triton-X-100, pH 7.4) for 30 minutes at room temperature. The lysates were centrifuged for 10 minutes at 12000rpm in a 4°C eppendorf microcentrifuge [Model MC 12V, manufactured by DU PONT DE NEMOURS and Co. (Inc.), Newtown, Conn, 06470, USA] to remove insoluble material. Separately, 20 μg of anti-integrin- α_M unconjugated monoclonal antibody, M1/70, was added to each lysate and incubated overnight at 4°C on a vortex shaker (Scientific industries Inc., Bohemia, N.Y., USA). The lysate-antibody mixtures were centrifuged at 12000rpm for 10 minutes in a microcentrifuge. A volume of about 170 μl of each supernatant was incubated with 70 μl

of washed protein G-beads (Pierce, Maridian road, Rockford, IL, USA) for 2 hours at 4°C on a vortex shaker. The beads were washed trice with immunoprecipitation buffer and antigen-antibody complexes were eluted with an appropriate volume of protein sample buffer. Alongside the immunoprecipitates, equal amounts of pure lysate and supernatant from each sample were analyzed on a 7% SDS-PAGE under non-denaturing conditions. The gel was Coomassie-stained as in 4.7, and dried in a slap gel drier. The gel was then exposed to a Cyclon phosphor-imager for over a week. A one-phase exponential graph of molecular weight against migration distance was plotted for each band of the precision stain marker and an approximate molecular weight was calculated for each subunit of the immunoprecipitated dimer by interpolation.

4.15 Filtration of medium from *M. avium*-infected cells and transfer onto non-infected cells

The effect of medium from *M. avium*-infected cells on surface expression of either integrin- β_2 or integrin- α_M on non-infected cells was tested by filtering one-day-old medium from *M. avium*-infected cells and transferring onto non-infected cells for over seven days. The infected cells were fed with fresh culture medium each day. The filtration was done using 0.2 μ m filter (Vivascience AG, Hannover, Germany). At day 7 after infection, both infected and medium-tested cells were surface-labelled with either ^3H -galactose or ^{14}C -galactose and the membrane proteins were isolated as described in 4.5. The labelled membrane proteins from both cell types were mixed and analysed on gradient SDS-PAGE as in 4.6.1. The lane was cut and subjected to trypsin ingel digestion as in 4.9 to determine the distribution of radioactivity across the gel.